International Journal of Robust and Nonlinear Control

WILEY

RESEARCH ARTICLE OPEN ACCESS

Distributed SE(d) Formation Control of Multi-Agent Systems Using Relative Measurements

Chunlai Peng[1] | Kazunori Sakurama[2] | Nichika Miyano[1] | Mitsuhiro Yamazumi[3] | Taiga Sugawara[2]

[1]Graduate School of Informatics, Kyoto University, Kyoto, Japan | [2]Graduate School of Science Engineering, Osaka University, Osaka, Japan | [3]Advanced Technology R&D Center, Mitsubishi Electric Corporation, Hyogo, Japan

Correspondence: Kazunori Sakurama (sakurama.kazunori.es@osaka-u.ac.jp)

Received: 21 May 2024 | **Revised:** 6 July 2025 | **Accepted:** 20 July 2025

Funding: This work was supported in part by Japan Society for the Promotion of Science KAKENHI Grant Nos. 23K22781 and 23H04468, and the project of Theory of Innovative Mechanical Systems, collaborated by Kyoto University and Mitsubishi Electric Corporation.

Keywords: distributed control | formation control | multiagent systems | pose control | relative measurement

ABSTRACT

This study develops a solution to the distributed SE(d) formation control problem of multi-agent systems using only relative measurements between agents. In this problem, poses, that is, orientations and positions, of the agents are expected to achieve desired ones. We assume that each agent can only measure its neighbors' relative poses, and that communication between agents is unavailable. To address this problem, a fully distributed and relative controller is proposed to ensure achieving the control objective. We employ the gradient-flow method with a clique-based objective function to achieve the best performance of the distributed, gradient-based controller. Subsequently, a network condition for achieving this objective is the connectedness. The proposed method ensures the stationary center of the agents and the minimum undesired equilibrium set, yielding short travel distances and a large attraction region, respectively. Furthermore, the proposed method outperforms the existing methods as evidenced by simulations in a two-dimensional space. In addition, the effectiveness of the proposed method is verified through a three-dimensional simulation. The proposed method shows potential for applications in drone swarm coordination, autonomous underwater vehicle formation, and mobile robot collaborative transportation when only local sensing is available while communication is limited.

1 | Introduction

A multi-agent system, comprising multiple decision-making agents, performs various tasks in a shared environment, such as collaborative surveillance and automated factories [1, 2]. In many scenarios, the agents must form a designated formation to manipulate an object collaboratively, to survey an unknown area, or for other tasks.

Formation control aims at driving agents to achieve prescribed constraints on their positions under limited information caused by the sensing capability [3–6]. In the case of distance-based formation control, inter-agent distances are prescribed as a desired formation. Agents are assumed to be able to sense only relative positions with regard to their neighbors [6]. To achieve the distance-based formation, the network topology between the agents must be rigid [7–9]. However, only the local convergence is ensured over rigid graphs when using the distance-based method. Moreover, undesired formation patterns may be obtained such that a part of the formation is flipped from the desired one. In contrast, [10, 11] proposed a new formation control scheme, referred to as clique-based formation control,

wherein cliques (i.e., complete subgraphs) were used to compute the control input, instead of using edges as conventional methods. This method overcomes the issue of undesired formation patterns, that is, flipping, of the distance-based formation control.

Several existing studies on the coordination problems of multi-agent systems address orientation control problems and pose formation control problems, involving both orientation and position control. They have a wide range of applications, such as multiple satellites for remote earth estimation [12], cooperative monitoring [13] and so forth. Orientation control problems have been investigated in [14–18]. References [14, 15] solved a distributed orientation synchronization problem for fixed/switched topologies, respectively, in both absolute and relative measurement cases. In the latter case, the initial orientation discrepancies are assumed to be less than $\pi/2$. Reference [16] proposed an energy-based orientation controller with alignment over a strongly connected graph, possibly with delay, which also has the same limitation of the initial orientation discrepancies. References [17, 18] proposed orientation control ensuring the almost global attraction. By combining orientation control with conventional formation control, pose formation control can be achieved. However, this approach does not handle the travel distances of the agents because orientation is controlled without feedback of positions, while the formation controller refers to orientations to determine the direction, which causes the drift of the agents. Consequently, the agents will travel long distances before convergence. On the other hand, the pose formation control was studied in [19–29]. References [19–21] proposed methods to estimate orientations to ensure global pose control, and [22] proposed a distributed control method with position estimation. These methods with estimation rely on network communication to exchange their estimations, which may suffer from radio interference and packet loss. As for communication-free pose formation control, [23, 24] considered dynamical multi-agent systems under an uncertain model/disturbance over a directed tree graph. Reference [25] also assumed a directed tree graph. Methods over a (directed) tree graph are not robust to the connection loss because if a part of the graph is broken, certain agents will be left behind. As for a more general graph, [26] considered a uniformly connected switching graph for agents in two-dimensional space, while [27] considered three-dimensional space. Reference [28] proposed a pose formation control method over a connected graph with the consideration of a vision image. Reference [29] treated kinetic models of agents over a delay graph. These pose formation control methods have the same issue to the combination of the position and orientation control methods; that is, orientations are controlled without feedback on positions, resulting in long travel distances. Furthermore, most approaches have a limit on initial orientation discrepancies. The bearing-based approach has been taken for pose formation control [30, 31]. The prescribed formation is given by the bearing and orientation of the agents, and the prescription of the formation is less than that of our target, the pose (position and orientation).

Therefore, it is still significant to design a distributed pose formation controller only with relative measurements that do not need network communication to ensure (i) short travel distances of the agents and (ii) a large attraction region. To obtain both properties, we employ the gradient-based method with a clique-based objective function involving orientation and position discrepancies. The important property of clique-based objective functions is that a gradient-based controller is distributed if and only if its objective function is clique-based [10]. Hence, a distributed gradient-based controller can perform the best only if it is based on clique-based functions, not edge-based functions. The proposed method performs the best in that the volume of the undesired equilibrium set is the smallest among gradient-based methods. Gradient-based methods generally provide undesired equilibrium points, where the formation is not achieved while the objective function is minimized. Because of the minimum undesired equilibrium set, the proposed method is expected to provide (ii) a large attraction region. Furthermore, the proposed clique-based controller involves not only orientation but also position discrepancies among cliques to determine control input. This structure ensures the efficient movement of the agents by restraining drift, which keeps the center of the agent positions stationary and consequently leads to (i) short travel distances. In contrast, conventional edge-based controllers do not restrain drift, causing unnecessary movement and resulting in longer travel distances. Notably, this article first provides a theoretical evaluation of drift in pose formation control and shows that our method minimizes drift by incorporating orientation and position discrepancies across cliques.

First, we formulate the pose formation control problem by providing the discrepancy between the current and desired poses over SE(d), that is, the special Euclidean space. Subsequently, we construct a clique-based objective function to evaluate the pose errors, that is, the orientation and position discrepancies in a unified way. Thereafter, a distributed controller is designed from the gradient of the function, requiring only relative measurements. Here, the conventional pattern matching technique is improved to consider the discrepancy of the orientation and position in a unified manner. We show that the best performance is achieved among the distributed, gradient-based controllers because of the clique-based objective function. We guarantee that the desired configuration is locally attractive and the center of the agent positions does not move. Finally, we demonstrate the effectiveness of the proposed method through numerical experiments via comparison with existing methods. The advantages mentioned above are demonstrated through simulations in various settings. (i) The travel distances of the agents of the proposed method are significantly shorter than those of the other methods. (ii) The success rate of the proposed method is 100%, which indicates a large attraction region. Note that the proposed distributed controller requires only relative measurements, not absolute measurements or network communication. Prominent real-world scenarios include autonomous drone swarms in GNSS (Global Navigation Satellite Systems)-denied environments, such as indoor exploration or disaster response, where onboard vision or LiDAR (Light Detection and Ranging) is used to estimate neighboring drones' poses. Another critical case involves underwater vehicle teams conducting seabed mapping in that acoustic-based relative sensing is available, but inter-agent communication remains unreliable.

A part of the results in this article has been presented in the authors' conference paper [32]. The differences from the conference version are as follows. First, the attractiveness of the desired configuration is theoretically proved. Second, a gradient-flow

method for systems over SE(d) is developed in a general manner. Third, simulation results are compared with existing methods, and a simulation in three-dimensional space is conducted. Compared with the authors' previous study [10, 11, 33, 34], the present article considers the desired orientations in the control objective and the system over SE(d). Consequently, the range of applications of this study becomes wider, including target monitoring, cooperative transport, and attitude synchronization.

The remainder of this article is organized as follows. In Section 2, we briefly introduce the notations and preliminaries of the article. The problem formulation is stated in Section 3. In Section 4, as a solution to this problem, a gradient-based, distributed controller is designed. Section 5 presents the simulation results to verify the effectiveness of the designed controller. The conclusions are presented in Section 6.

2 | Preliminary

2.1 | Notation

Let $\mathbb{R}$ and $\mathbb{R}_+$ be the set of the real numbers and the set of the non-negative real numbers, respectively. The orthogonal group, denoted as $\mathrm{O}(d)$, is the set of $d \times d$ orthogonal matrices. Let $\mathrm{SO}(d) \subset \mathbb{R}^{d\times d}$ denote the set of the d-dimensional orthogonal matrices with determinant of 1, and the Euclidean group of dimension d is represented by $\mathrm{SE}(d) = \mathrm{SO}(d) \times \mathbb{R}^d$. The Lie algebra of $\mathrm{SE}(d)$ is denoted as $\mathrm{se}(d) = \mathrm{skew}(d) \times \mathbb{R}^d$. $\hat{R}(R, x) = (\hat{R}R, \hat{R}x)$ is defined as the multiplication of $\hat{R} \in \mathrm{SO}(d)$ and $(R, x) \in \mathrm{SE}(d)$. For a square matrix, the trace and the determinant are denoted by $\mathrm{tr}(\cdot)$ and $\det(\cdot)$, respectively. Let $\mathrm{skew}(d) \in \mathbb{R}^{d\times d}$ denote the set of the d-dimensional skew-symmetric matrices, and $\mathcal{P}_{\mathrm{skew}} : \mathbb{R}^{d\times d} \to \mathbb{R}^{d\times d}$ be the orthogonal projection onto the set of skew-symmetric matrices, that is, for a matrix $X \in \mathbb{R}^{d\times d}$,

$$\mathcal{P}_{\mathrm{skew}}(X) = \frac{1}{2}(X - X^\top) \tag{1}$$

The block diagonal matrix of two matrices X_1 and X_2 is denoted as $\mathrm{diag}(X_1, X_2)$. The kernel of a function $f : \mathcal{X} \to \mathbb{R}^m$ is represented as $f^{-1}(0) = \{x \in \mathcal{X} : f(x) = 0\}$. Let $(x_i)_{i\in\mathcal{N}}$ denote the n-tuple comprising x_i for $i \in \mathcal{N}$ as

$$(x_i)_{i\in\mathcal{N}} = (x_1, x_2, \ldots, x_n)$$

where $\mathcal{N} = \{1, 2, \ldots, n\}$. The average of an n-tuple $(x_i)_{i\in\mathcal{N}}$ is denoted with $\mathrm{avg}(\cdot)$ as follows:

$$\mathrm{avg}((x_i)_{i\in\mathcal{N}}) = \frac{1}{n}\sum_{i\in\mathcal{N}} x_i$$

The inner product of matrix-vector pairs $(M_1, v_1), (M_2, v_2) \in \mathbb{R}^{d\times d} \times \mathbb{R}^d$ weighted by a pair of positive constants (κ_M, κ_v) is defined as

$$\langle (M_1, v_1), (M_2, v_2) \rangle_{(\kappa_M,\kappa_v)} = \kappa_M \mathrm{tr}(M_1^\top M_2) + \kappa_v v_1^\top v_2$$

The norm of $(M, v) \in \mathbb{R}^{d\times d} \times \mathbb{R}^d$ weighted by (κ_M, κ_v) is defined as

$$\|(M, v)\|_{(\kappa_M,\kappa_v)} = \sqrt{\langle (M, v), (M, v) \rangle_{(\kappa_M,\kappa_v)}}$$

The distance of a tuple $(M_i, v_i)_{i\in\mathcal{N}} \in (\mathbb{R}^{d\times d} \times \mathbb{R}^d)^n$ and a set $\mathcal{D} \subset (\mathbb{R}^{d\times d} \times \mathbb{R}^d)^n$ weighted by (κ_M, κ_v) is defined as

$$\begin{aligned}&\mathrm{dist}_{(\kappa_M,\kappa_v)}((M_i, v_i)_{i\in\mathcal{N}}, \mathcal{D}) \\ &= \inf_{(\hat{M}_i,\hat{v}_i)_{i\in\mathcal{N}}\in\mathcal{D}} \sum_{i\in\mathcal{N}} \sqrt{\|(M_i - \hat{M}_i, v_i - \hat{v}_i)\|^2_{(\kappa_M,\kappa_v)}}\end{aligned} \tag{2}$$

Let $\mathrm{pow}(\cdot)$ denote the power set of a set. For a set $C \subset \{1, 2, \ldots, n\}$, let $\mathcal{P}_C : \mathrm{pow}((\mathrm{SE}(d))^n) \to \mathrm{pow}((\mathrm{SE}(d))^{|C|})$ be the projection of a set onto the $(R_i, x_i)_{i\in C}$ space, namely, for a set $\mathcal{D} \subset (\mathrm{SE}(d))^n$

$$\begin{aligned}\mathcal{P}_C(\mathcal{D}) = \{(R_i, x_i)_{i\in C} \in (\mathrm{SE}(d))^{|C|} : \exists (R_i, x_i)_{i\in\mathcal{N}\setminus C} \\ \text{s.t.} (R_i, x_i)_{i\in\mathcal{N}} \in \mathcal{D}\}\end{aligned} \tag{3}$$

2.2 | Interaction Topology

Consider an undirected graph represented by a pair $G = (\mathcal{V}, \mathcal{E})$, where $\mathcal{V} = \{1, \ldots, n\}$ is a vertex set, and $\mathcal{E} \subseteq \mathcal{V} \times \mathcal{V}$ is a set comprising edges. Adjacent vertices are referred to as neighbors. The set of the neighbors of vertex i is represented by $\mathcal{N}_i = \{j \in \mathcal{V} : (i, j) \in \mathcal{E}\}$. The graph G is considered complete if every pair of distinct vertices is adjacent to each other. The induced graph of G is a graph with a vertex set $C \subset \mathcal{V}$ and the edge set comprising the edges $(i, j) \in \mathcal{E}$ satisfying $i, j \in C$. An induced subgraph is considered a clique if the subgraph is complete. The number of the vertices in a clique C is denoted by $|C|$. Clique C is maximal if it is not contained in any other cliques in G. The set of all the maximal cliques in G is denoted by $\mathrm{clq}(G) \subset \mathrm{pow}(\mathcal{V})$, and let $\mathrm{clq}_i(G) = \{C \in \mathrm{clq}(G) : i \in C\}$ be the subset of the maximal cliques to which vertex i belongs.

Example 1. Consider the graph $G = (\mathcal{N}, \mathcal{E})$ in Figure 1. The set of maximal cliques in G is given as

$$\mathrm{clq}(G) = \{\{1, 2\}, \{2, 3, 4\}, \{3, 4, 5, 6\}\}$$

The subset of the maximal cliques that each node belongs to is given as

$$\begin{aligned}&\mathrm{clq}_1(G) = \{\{1, 2\}\},\ \mathrm{clq}_2(G) = \{\{1, 2\}, \{2, 3, 4\}\}, \\ &\mathrm{clq}_3(G) = \mathrm{clq}_4(G) = \{\{2, 3, 4\}, \{3, 4, 5, 6\}\}, \\ &\mathrm{clq}_5(G) = \mathrm{clq}_6(G) = \{\{3, 4, 5, 6\}\}\end{aligned}$$

The maximal cliques to which a vertex belongs form the set of its neighbors as follows.

Lemma 1 ([34]). *For a graph G, the following holds*:

$$\bigcup_{C\in\mathrm{clq}_i(G)} C = \mathcal{N}_i \tag{4}$$

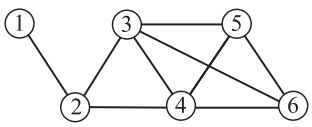

FIGURE 1 | Example of a graph.

2.3 | Pattern Matching

The pattern matching technique has been studied in [35]. Here, we introduce a conventional result, which is crucial to the formation control [11]. For vectors $x_i,\ x_i^* \in \mathbb{R}^d, i \in \mathcal{V} = \{1, 2, \ldots, n\}$, consider the optimization problem

$$\min_{(\hat{R},\hat{\tau})\in \mathrm{SE}(d)} \sum_{i=1}^{n} \|x_i - (\hat{R}x_i^* + \hat{\tau})\|^2 \tag{5}$$

The singular value decomposition is considered as

$$\sum_{i=1}^{n} x_i^* x_i^\top = USV^\top \tag{6}$$

with matrices $S = \mathrm{diag}(\sigma_1, \ldots, \sigma_d),\ \sigma_1 \geq \sigma_2 \geq \cdots \geq \sigma_d \geq 0$, $U,\ V \in \mathrm{SO}(d)$. The solution of the problem (5) is derived as follows:

$$\begin{cases} \hat{R} = V\,\mathrm{diag}(\underbrace{1, \ldots, 1}_{d-1}, \det(VU^\top))U^\top \\ \hat{\tau} = \mathrm{avg}((x_k)_{k\in\mathcal{V}}) - \hat{R}\,\mathrm{avg}((x_k^*)_{k\in\mathcal{V}}) \end{cases} \tag{7}$$

3 | Problem Statement

3.1 | System Model

Consider n mobile agents in d-dimensional space $\mathbb{R}^d$, whose indexes are represented by a set $\mathcal{V} = \{1, 2, \ldots, n\}$. The global coordinate frame is denoted by Σ, and the local coordinate frame of agent $i \in \mathcal{V}$ at time t is denoted by $\Sigma_i(t)$. Let $x_i(t) \in \mathbb{R}^d$ and $R_i(t) \in \mathrm{SO}(d)$ be the position and orientation of agent i with respect to Σ, respectively. Let $x_j^{[i]}(t) \in \mathbb{R}^d$ and $R_j^{[i]}(t) \in \mathrm{SO}(d)$ represent the relative position and relative orientation of agent $j \in \mathcal{N}_i$ with respect to the local coordinate frame $\Sigma_i(t)$, respectively. The variables defined in $\Sigma_i(t)$ are denoted with the superscript $[i]$. We refer to $(R_i(t), x_i(t)) \in \mathrm{SE}(d)$ and $(R_j^{[i]}(t), x_j^{[i]}(t)) \in \mathrm{SE}(d)$ as the absolute and relative poses, respectively. These variables satisfy

$$\begin{bmatrix} R_j^{[i]}(t) & x_j^{[i]}(t) \\ 0 & 1 \end{bmatrix} = \begin{bmatrix} R_i(t) & x_i(t) \\ 0 & 1 \end{bmatrix}^{-1} \begin{bmatrix} R_j(t) & x_j(t) \\ 0 & 1 \end{bmatrix} \tag{8}$$

Let $(S_i(t), u_i(t)) \in \mathrm{se}(d)$ be the control input of agent i. The control inputs $u_i(t)$ and $S_i(t)$ correspond to the velocity and angular velocity commands, respectively. Agent i is governed by the kinematic model

$$\begin{bmatrix} \dot{R}_i(t) & \dot{x}_i(t) \\ 0 & 0 \end{bmatrix} = \begin{bmatrix} R_i(t) & x_i(t) \\ 0 & 1 \end{bmatrix} \begin{bmatrix} S_i(t) & u_i(t) \\ 0 & 0 \end{bmatrix} \tag{9}$$

which is a differential equation of $(R_i(t), x_i(t)) \in \mathrm{SE}(d)$ [36].

For the two-dimensional space, Figure 2 illustrates the transformation between the frames Σ and $\Sigma_i(t)$. Let $\theta_i(t) \in [0, 2\pi)$ be the orientation angle of agent i with regard to Σ, and let $\omega(t) \in \mathbb{R}^d$ denote the angular velocity of agent i. Then, the orientation matrix $R_i(t)$ and angular control input $S_i(t)$ can be expressed as follow:

$$R_i(t) = \begin{bmatrix} \cos\theta_i(t) & -\sin\theta_i(t) \\ \sin\theta_i(t) & \cos\theta_i(t) \end{bmatrix},\ S_i(t) = \begin{bmatrix} 0 & -\omega_i(t) \\ \omega_i(t) & 0 \end{bmatrix}$$

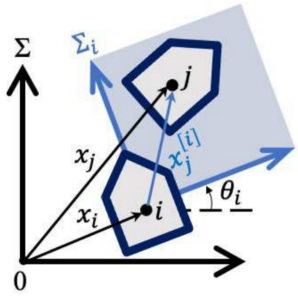

FIGURE 2 | Transformation between the global frame Σ and local frame Σ_i $(d = 2)$.

Consequently, (9) is reduced to

$$\begin{cases} \dot{\theta}_i(t) = \omega_i(t) \\ \dot{x}_i(t) = R_i(t)u_i(t) \end{cases}$$

3.2 | Control Objective

In this study, agents are expected to achieve a desired formation shape with desired directions. This control objective is formulated as follows:

$$\lim_{t\to\infty}\left(\begin{bmatrix} R_j^{[i]}(t) & x_j^{[i]}(t) \\ 0 & 1 \end{bmatrix} - \begin{bmatrix} {}^*R_j^{[i]} & {}^*x_j^{[i]} \\ 0 & 1 \end{bmatrix} \right) = 0 \quad \forall i, j \in \mathcal{V} \tag{10}$$

where $({}^*R_j^{[i]}, {}^*x_j^{[i]}) \in \mathrm{SE}(d)$ is the desired relative pose between agents i and j. Assume that $({}^*R_j^{[i]}, {}^*x_j^{[i]})_{i,j\in\mathcal{V}}$ is realizable according to (8), that is, there exists $(R_i^*, x_i^*)_{i\in\mathcal{V}} \in (\mathrm{SE}(d))^n$ such that

$$\begin{bmatrix} {}^*R_j^{[i]} & {}^*x_j^{[i]} \\ 0 & 1 \end{bmatrix} = \begin{bmatrix} R_i^* & x_i^* \\ 0 & 1 \end{bmatrix}^{-1} \begin{bmatrix} R_j^* & x_j^* \\ 0 & 1 \end{bmatrix} \quad \forall i, j \in \mathcal{V} \tag{11}$$

Using Equations (8) and (11), the control objective (10) can be formulated based on the attractiveness of $\mathcal{T}((R_i^*, x_i^*)_{i\in\mathcal{V}})$, where

$$\begin{aligned} \mathcal{T}((R_i^*, x_i^*)_{i\in\mathcal{V}}) = \{(R_i, x_i)_{i\in\mathcal{V}} \in (\mathrm{SE}(d))^n :\ & \exists(\hat{R}, \hat{\tau}) \in \mathrm{SE}(d) \\ \text{s.t.} & \begin{bmatrix} R_i & x_i \\ 0 & 1 \end{bmatrix} = \begin{bmatrix} \hat{R} & \hat{\tau} \\ 0 & 1 \end{bmatrix} \begin{bmatrix} R_i^* & x_i^* \\ 0 & 1 \end{bmatrix} \ \forall i \in \mathcal{V}\} \end{aligned} \tag{12}$$

Here, $\mathcal{T}((R_i^*, x_i^*)_{i\in\mathcal{V}})$ is considered as locally attractive if there exists an open set $\mathcal{M} \supset \mathcal{T}((R_i^*, x_i^*)_{i\in\mathcal{V}})$ such that

$$\begin{aligned} &\lim_{t\to\infty} \mathrm{dist}((R_i(t), x_i(t))_{i\in\mathcal{V}}, \mathcal{T}((R_i^*, x_i^*)_{i\in\mathcal{V}})) = 0 \\ &\forall (R_i(0), x_i(0))_{i\in\mathcal{V}} \in \mathcal{M} \end{aligned} \tag{13}$$

On the other hand, it is expected that the agents will remain as still as possible. For this purpose, we require that the center of the agent positions is stationary, that is, the following holds:

$$\frac{1}{n}\sum_{i\in\mathcal{V}} x_i(t) = \frac{1}{n}\sum_{i\in\mathcal{V}} x_i(0) \tag{14}$$

See Figure 3 for an example of the control objective (10), where (a) gives the desired poses, (b) shows the motions of the agents with the stationary center in Equation (14), and (c) shows those without the stationary center.

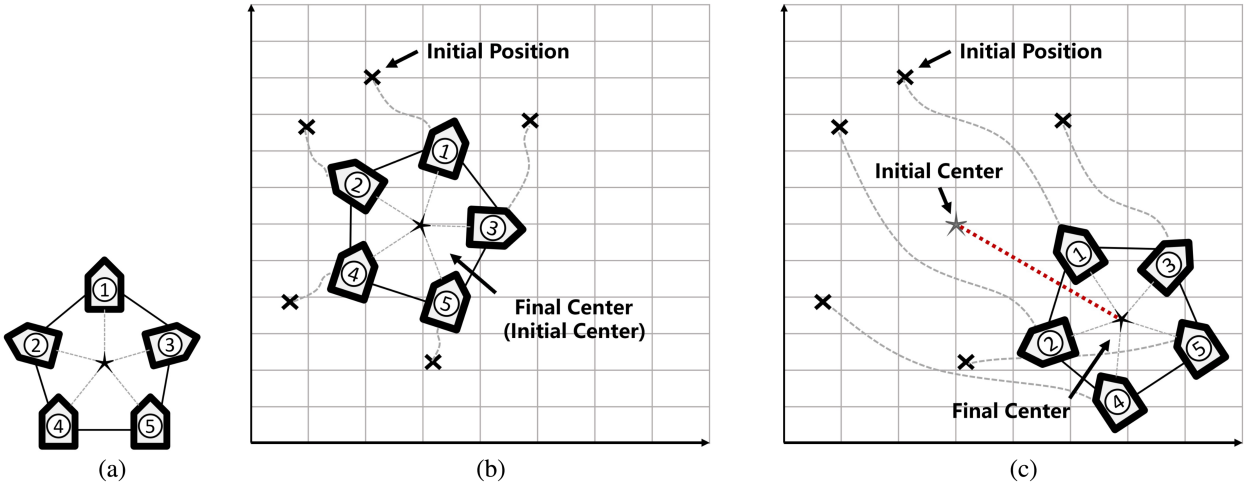

FIGURE 3 | Examples of the control objective: (a) The desired poses, (b) the motions of the agents with the stationary center, and (c) those without the stationary center.

3.3 | Admissible Controllers

Consider the undirected and time-invariant graph G describing the sensing network of the agents. Agent $i \in \mathcal{V}$ can measure the relative poses $(R_j^{[i]}(t), x_j^{[i]}(t))$ only to its neighbors $j \in \mathcal{N}_i$. In terms of information on the desired configuration, agent i knows the desired relative pose $({}^* R_j^{[i]}, {}^* x_j^{[i]})$ only to its neighbors $j \in \mathcal{N}_i$. Consequently, the control input $(S_i(t), u_i(t))$ for agent i must be generated as

$$\begin{cases} S_i(t) = F_i((R_j^{[i]}(t), x_j^{[i]}(t), {}^* R_j^{[i]}, {}^* x_j^{[i]})_{j\in\mathcal{N}_i}) \\ u_i(t) = f_i((R_j^{[i]}(t), x_j^{[i]}(t), {}^* R_j^{[i]}, {}^* x_j^{[i]})_{j\in\mathcal{N}_i}) \end{cases} \tag{15}$$

where $F_i : (\mathrm{SE}(d) \times \mathrm{SE}(d))^{|\mathcal{N}_i|} \to \mathrm{skew}(d)$ and $f_i : (\mathrm{SE}(d) \times \mathrm{SE}(d))^{|\mathcal{N}_i|} \to \mathbb{R}^d$. The functions F_i and f_i in Equation (15) are referred to as distributed and relative controllers as they only depend on local information on neighbors. We assume that only this type of controller is admissible.

When implementing the controller (15), agent i requires the relative pose $(R_j^{[i]}(t), x_j^{[i]}(t))$ in the local frame Σ_i, which can be obtained by using onboard sensors, for example, camera, LiDAR, and acoustic-based sensor, equipped with agent i.

3.4 | Gradient-Flow Method for SE(d) Multi-Agent System

We employ the gradient-flow method for the system (9). Let $v : (\mathrm{SE}(d))^n \to \mathbb{R}_+$ be an objective function of $(R_i, x_i)_{i\in\mathcal{V}}$ which takes the global minimum zero when $(R_i, x_i)_{i\in\mathcal{V}}$ is desired. The controllers are designed according to the gradient as follows:

$$\begin{cases} S_i(t) = -\mathcal{P}_{\mathrm{skew}}(R_i^\top(t)\frac{\partial v}{\partial R_i}(R_i(t), x_i(t))_{i\in\mathcal{V}}) \\ u_i(t) = -R_i^\top(t)\frac{\partial v}{\partial x_i}((R_i(t), x_i(t))_{i\in\mathcal{V}}) \end{cases} \tag{16}$$

Consequently, the zero set $v^{-1}(0)$ is attractive under certain conditions.

Lemma 2. *Consider the system (9) with the gradient-based controller (16) for a differentiable function $v : (\mathrm{SE}(d))^n \to \mathbb{R}_+$. Assume that $(R_i(t), x_i(t)) \in \mathrm{SE}(d)$ is bounded for all $i \in \mathcal{V}$ and there exists an open set $\mathcal{O} \supset v^{-1}(0)$ such that*

$$((\mathcal{P}_{\mathrm{skew}}(R_i^\top \frac{\partial v}{\partial R_i}), \frac{\partial v}{\partial x_i})_{i\in\mathcal{V}})^{-1}(0) \cap \mathcal{O} = v^{-1}(0) \tag{17}$$

Then, the zero set $v^{-1}(0)$ is locally attractive.

Proof. See Appendix A. □

Assume that $v^{-1}(0)$ is locally attractive. Then, to achieve the control objective, the local attractiveness (13) of $\mathcal{T}((R_i^*, x_i^*)_{i\in\mathcal{V}})$, we must design an objective function $v((R_i, x_i)_{i\in\mathcal{V}})$ such that

$$v^{-1}(0) = \mathcal{T}((R_i^*, x_i^*)_{i\in\mathcal{V}}) \tag{18}$$

On the other hand, the gradient-based controllers (16) are expected to be distributed and relative, that is, the function v must satisfy the following condition from Equation (15).

Request 1: There exist functions $F_i : (\mathrm{SE}(d) \times \mathrm{SE}(d))^{|\mathcal{N}_i|} \to \mathrm{skew}(d)$ and $f_i : (\mathrm{SE}(d) \times \mathrm{SE}(d))^{|\mathcal{N}_i|} \to \mathbb{R}^d$ such that

$$\begin{cases} F_i((R_j^{[i]}, x_j^{[i]}, {}^* R_j^{[i]}, {}^* x_j^{[i]})_{j\in\mathcal{N}_i}) = -\mathcal{P}_{\mathrm{skew}}(R_i^\top \frac{\partial v}{\partial R_i}((R_i, x_i)_{i\in\mathcal{V}})) \\ f_i((R_j^{[i]}, x_j^{[i]}, {}^* R_j^{[i]}, {}^* x_j^{[i]})_{j\in\mathcal{N}_i}) = -\frac{\partial v}{\partial x_i}((R_i, x_i)_{i\in\mathcal{V}}) \end{cases} \tag{19}$$

where $(R_j^{[i]}, x_j^{[i]})$ is obtained from (R_i, x_i) and (R_j, x_j) as

$$\begin{bmatrix} R_j^{[i]} & x_j^{[i]} \\ 0 & 1 \end{bmatrix} = \begin{bmatrix} R_i & x_i \\ 0 & 1 \end{bmatrix}^{-1} \begin{bmatrix} R_j & x_j \\ 0 & 1 \end{bmatrix}$$

according to (8).

3.5 | Problem Setting

Note that (18) and (19) may be incompatible. In other words, there may not exist a distributed and relative controller (15)

such that the control objective (13) is attained. The compatibility depends on the topology of the graph G. Thus, we consider relaxing the control objective (13), the attractiveness of $\mathcal{T}((R_i^*, x_i^*)_{i\in\mathcal{V}})$, to that of the zero set $v^{-1}(0)$ for an admissible function $v \in \mathcal{A}((R_i^*, x_i^*)_{i\in\mathcal{V}}, G)$ approximating to $\mathcal{T}((R_i^*, x_i^*)_{i\in\mathcal{V}})$. Here, $\mathcal{A}((R_i^*, x_i^*)_{i\in\mathcal{V}}, G)$ is the set of the differentiable functions $v : (\mathrm{SE}(d))^n \to \mathbb{R}_+$ satisfying Request 1 and

$$v((R_i, x_i)_{i\in\mathcal{V}}) = 0 \text{ for } (R_i, x_i)_{i\in\mathcal{V}} \in \mathcal{T}((R_i^*, x_i^*)_{i\in\mathcal{V}}) \tag{20}$$

Among these functions, we expect to obtain the best approximate function $v_\star \in \mathcal{A}((R_i^*, x_i^*)_{i\in\mathcal{V}}, G)$ to $\mathcal{T}((R_i^*, x_i^*)_{i\in\mathcal{V}})$, defined as

$$v_\star^{-1}(0) \subset v^{-1}(0) \quad \forall v \in \mathcal{A}((R_i^*, x_i^*)_{i\in\mathcal{V}}, G) \tag{21}$$

Problem 1. Determine the best approximate function $v_\star \in \mathcal{A}((R_i^*, x_i^*)_{i\in\mathcal{V}}, G)$ to $\mathcal{T}((R_i^*, x_i^*)_{i\in\mathcal{V}})$ in Equation (21) whose gradient-based controller (16) generates distributed and relative controllers (15) satisfying (14).

Notably, the controller designed with $v_\star$ offers the best performance in that its undesired equilibrium set $\mathcal{T}((R_i^*, x_i^*)_{i\in\mathcal{V}}) \setminus v_\star^{-1}(0)$ is smaller than those of any other controllers $\mathcal{T}((R_i^*, x_i^*)_{i\in\mathcal{V}}) \setminus v^{-1}(0)$ from Equation (21).

Next, we specify a condition of G to attain (13).

Problem 2. Specify the topology of the graph G such that $\mathcal{T}((R_i^*, x_i^*)_{i\in\mathcal{V}})$ is locally attractive with a distributed and relative controller.

4 | Main Result

4.1 | Solution to Problem 1

First, we present a candidate for the best approximate function inspired from the authors' previous study [34].

Lemma 3 ([34]). *The following function satisfies (21):*

$$v_\star((R_i, x_i)_{i\in\mathcal{V}}) = \sum_{C\in\mathrm{clq}(G)} v_C((R_j, x_j)_{j\in C}) \tag{22}$$

with

$$v_C((R_j, x_j)_{j\in C}) = \frac{1}{2}(\mathrm{dist}_{(\kappa_M,\kappa_v)}((R_j, x_j)_{j\in C}, \mathcal{P}_C(\mathcal{T}((R_j^*, x_j^*)_{j\in\mathcal{V}}))))^2 \tag{23}$$

for positive constants κ_M, κ_v.

Notably, the partial derivative of $v_\star$ with respect to the variable of each agent is always distributed, that is,

$$\left(\frac{\partial v_\star}{\partial R_i}((R_i, x_i)_{i\in\mathcal{V}}), \frac{\partial v_\star}{\partial x_i}((R_i, x_i)_{i\in\mathcal{V}})\right) = \left(\sum_{C\in\mathrm{clq}_i(G)} \frac{\partial v_C}{\partial R_i}((R_j, x_j)_{j\in C}), \sum_{C\in\mathrm{clq}_i(G)} \frac{\partial v_C}{\partial x_i}((R_j, x_j)_{j\in C})\right)$$

depends only on the agent own and its neighbors states $(R_j, x_j)_{j\in\mathcal{N}_i}$ from Equation (4) in Lemma 1. Hence, the gradient-based controller (16) of (22) is distributed. Furthermore, Lemma 3 guarantees that $v_\star$ in Equation (22) is the best approximate function to $\mathcal{T}((R_i^*, x_i^*)_{i\in\mathcal{V}})$ if $v_\star \in \mathcal{A}((R_i^*, x_i^*)_{i\in\mathcal{V}}, G)$; that is, it satisfies (19) and (20). Because (20) can be easily verified, we confirm just (19). For this, we calculate its right-hand side with $v_\star$ in Equation (22), where the gradient of v_C in Equation (23) has to be derived. Using Equations (3) and (12), the projection in Equation (22) is calculated as

$$\begin{aligned}\mathcal{P}_C(\mathcal{T}((R_j^*, x_j^*)_{j\in\mathcal{V}})) &= \{(R_j, x_j)_{j\in C} \in (\mathrm{SE}(d))^{|C|} : \exists(\hat{R}_C, \hat{\tau}_C) \in \mathrm{SE}(d) \\ &\quad \text{s.t.} \begin{bmatrix} R_j & x_j \\ 0 & 1 \end{bmatrix} = \begin{bmatrix} \hat{R}_C & \hat{\tau}_C \\ 0 & 1 \end{bmatrix} \begin{bmatrix} R_j^* & x_j^* \\ 0 & 1 \end{bmatrix} \forall j \in C\}\end{aligned} \tag{24}$$

Using Equations (2) and (24), (23) is reduced to

$$v_C((R_j, x_j)_{j\in C}) = \hat{v}_C((R_j, x_j, R_j^*, x_j^*)_{j\in C}) \tag{25}$$

where

$$\begin{aligned}&\hat{v}_C((R_j, x_j, R_j^*, x_j^*)_{j\in C}) \\ &= \frac{1}{2}\min_{(\hat{R}_C,\hat{\tau}_C)\in\mathrm{SE}(d)} \sum_{j\in C} \left\|(R_j - \tilde{R}_j, x_j - \tilde{x}_j)\right\|^2_{(\kappa_M,\kappa_v)} \\ &\text{for } \begin{bmatrix} \tilde{R}_j & \tilde{x}_j \\ 0 & 1 \end{bmatrix} = \begin{bmatrix} \hat{R}_C & \hat{\tau}_C \\ 0 & 1 \end{bmatrix} \begin{bmatrix} R_j^* & x_j^* \\ 0 & 1 \end{bmatrix}\end{aligned} \tag{26}$$

The optimization problem in Equation (26) is similar to the problem (5) in Section 2.3. The difference is that (5) evaluates only the position discrepancy while (26) does the pose discrepancy. We can solve (26) using the technique for (5) as follows.

Lemma 4. *For positive constants κ_M, κ_v, the solution $(\hat{R}_C, \hat{\tau}_C)$ to the optimization problem in the right-side hand of (26) is expressed as*

$$\begin{cases} \hat{R}_C = \hat{V}\,\mathrm{diag}(\underbrace{1, \ldots, 1}_{d-1}, \det(\hat{V}\hat{U}^\top))\hat{U}^\top \\ \hat{\tau}_C = \mathrm{avg}((x_k)_{k\in C}) - \hat{R}_C\mathrm{avg}((x_k^*)_{k\in C}) \end{cases} \tag{27}$$

where orthogonal matrices $\hat{U}$, $\hat{V} \in \mathrm{O}(d)$ satisfy the singular value decomposition

$$\sum_{j\in C}\{\kappa_v(x_j^* - \mathrm{avg}((x_k^*)_{k\in C}))(x_j - \mathrm{avg}((x_k)_{k\in C}))^\top + \kappa_M R_j^*(R_j)^\top\} = \hat{U}\hat{S}\hat{V}^\top \tag{28}$$

with a diagonal matrix $\hat{S} = \mathrm{diag}(\sigma_1', \ldots, \sigma_d')$, and $\sigma_1' \geq \sigma_2' \geq \cdots \geq \sigma_d' \geq 0$.

Proof. See Appendix A. □

Consequently, the gradient of $\hat{v}_C$ in Equation (26) is calculated as follows.

Lemma 5. *For positive constants κ_M, κ_v, the following holds for $\hat{v}_C$ in Equation (26):*

$$\frac{\partial \hat{v}_C}{\partial R_i}((R_j, x_j, R_j^*, x_j^*)_{j\in C}) = \kappa_M(R_i - \hat{R}_C R_i^*) \tag{29}$$

$$\frac{\partial \hat{v}_C}{\partial x_i}((R_j, x_j, R_j^*, x_j^*)_{j\in C}) = \kappa_v(x_i - \mathrm{avg}((x_k)_{k\in C}) - \hat{R}_C(x_i^* - \mathrm{avg}((x_k^*)_{k\in C}))) \tag{30}$$

where $\hat{R}_C$ is expressed as (27).

Proof. See Appendix A. □

A significant property of the gradient of $\hat{v}_C$ in Equation (26) is the relativity, that is, the equivalence in terms of the pose transformation, as follows.

Lemma 6. *For positive constants κ_M, κ_v, the function $\hat{v}_C$ in Equation (26) satisfies the following for any $(R, \tau), (R^*, \tau^*) \in \mathrm{SE}(d)$:*

$$\frac{\partial \hat{v}_C}{\partial R_i}((R(R_j, x_j + \tau), R^*(R_j^*, x_j^* + \tau^*))_{j\in C}) = R\frac{\partial \hat{v}_C}{\partial R_i}((R_j, x_j, R_j^*, x_j^*)_{j\in C}) \tag{31}$$

$$\frac{\partial \hat{v}_C}{\partial x_i}((R(R_j, x_j + \tau), R^*(R_j^*, x_j^* + \tau^*))_{j\in C}) = R\frac{\partial \hat{v}_C}{\partial x_i}((R_j, x_j, R_j^*, x_j^*)_{j\in C}) \tag{32}$$

Proof. See Appendix A. □

Furthermore, the stationary center of the agents is guaranteed as follows.

Lemma 7. *Consider the system (9) with the gradient-based controller (16) for $v = v_\star$ in Equation (22). Then, (14) holds.*

Proof. See Appendix A. □

Accordingly, we can confirm that (19) holds and that the proposed controller (33) below is of the form (15) and is admissible. Furthermore, (14) is ensured by using this controller. Then, the solution to Problem 1 is obtained.

Theorem 1. *For positive constants κ_M, κ_v, the function $v_\star$ in Equation (22) belongs to $\mathcal{A}((R_i^*, x_i^*)_{i\in\mathcal{V}}, G)$ and is the best approximate function to $\mathcal{T}((R_i^*, x_i^*)_{i\in\mathcal{V}})$, that is, the designed controller performs the best in terms of the minimum undesired equilibrium set from Equation (21). The gradient-based controller (16) of $v = v_\star$ is relative and distributed in the form (15) for*

$$\begin{cases} F_i((R_j^{[i]}, x_j^{[i]}, {}^*R_j^{[i]}, {}^*x_j^{[i]})_{j\in\mathcal{N}_i}) = \kappa_M \sum_{C\in \mathrm{clq}_i(G)} \mathcal{P}_{\mathrm{skew}}(\hat{R}_C^{[i]}) \\ f_i((R_j^{[i]}, x_j^{[i]}, {}^*R_j^{[i]}, {}^*x_j^{[i]})_{j\in\mathcal{N}_i}) = \kappa_v \sum_{C\in \mathrm{clq}_i(G)} (\mathrm{avg}((x_j^{[i]})_{j\in C}) \\ \qquad\qquad -\hat{R}_C^{[i]}\mathrm{avg}(({}^*x_j^{[i]})_{j\in C})) \end{cases} \tag{33}$$

with constants κ_M, κ_v, and $(\hat{R}_C^{[i]}, \hat{\tau}_C^{[i]}) \in \mathrm{SE}(d)$ expressed as (27) and (28), where $\hat{R}_C, \hat{\tau}_C, R_j, x_j, x_k, R_j^*, x_j^*$, and x_k^* are replaced with $\hat{R}_C^{[i]}$, $\hat{\tau}_C^{[i]}$, $R_j^{[i]}$, $x_j^{[i]}$, $x_k^{[i]}$, ${}^*R_j^{[i]}$, ${}^*x_j^{[i]}$, and ${}^*x_k^{[i]}$, respectively. By using this controller, (14) holds.

Proof. Lemma 3 guarantees that the function $v_\star$ in Equation (22) is the best approximate function to $\mathcal{T}((R_i^*, x_i^*)_{i\in\mathcal{V}})$, that is, satisfies (21). The designed controller (33) is relative and distributed, that is, satisfies (15) because $(\hat{R}_C^{[i]}, \hat{\tau}_C^{[i]})$ is composed of $R_j^{[i]}$, $x_j^{[i]}$, ${}^*R_j^{[i]}$, and ${}^*x_j^{[i]}$ for $j \in \mathcal{N}_i$ from Equation (4) in Lemma 1.

We show that (19) holds for $v = v_\star$. Using Equations (8), (11), (29), and (31),

$$\begin{aligned} R_i^\top \frac{\partial \hat{v}_C}{\partial R_i}((R_j, x_j, R_j^*, x_j^*)_{j\in C}) &= \frac{\partial \hat{v}_C}{\partial R_i}((R_i^\top(R_j, x_j - x_i), (R_i^*)^\top(R_j^*, x_j^* - x_i^*))_{j\in C}) \\ &= \frac{\partial \hat{v}_C}{\partial R_i}((R_j^{[i]}, x_j^{[i]}, {}^*R_j^{[i]}, {}^*x_j^{[i]})_{j\in C}) \\ &= \kappa_M(R_i^{[i]} - \hat{R}_C^{[i]}{}^*R_i^{[i]}) = \kappa_M(I - \hat{R}_C^{[i]}) \end{aligned} \tag{34}$$

is obtained, where I is the identity matrix and $R_i^{[i]} = {}^*R_i^{[i]} = I$ is used. Using Equations (1), (25), and (34), the right-hand side of the first equation of (19) is reduced to that of (33).

The second equation of (33) is obtained similarly.

(14) follows Lemma 7. □

4.2 | Solution to Problem 2

We specify the topology of the graph G such that $\mathcal{T}((R_i^*, x_i^*)_{i\in\mathcal{V}})$ is locally attractive. According to Lemma 2, the attractiveness of the zero set $v^{-1}(0)$ is guaranteed under two conditions by using the gradient-based controller (16). Then, (18) is necessarily satisfied by the target function $v_\star$ in Equation (22). To satisfy this condition, the required topology of the graph G is proven to be connected.

Lemma 8. *For graph G and the set $\mathcal{T}((R_i^*, x_i^*)_{i\in\mathcal{V}})$ in Equation (12), $v_\star$ in Equation (22) satisfies (18) for $v = v_\star$ if and only if G is connected.*

Proof. See Appendix A. □

We confirm the two assumptions in Lemma 2.

Lemma 9. *Consider the system (9) with the gradient-based controller (16) for $v = v_\star$ in Equation (22). Then, $(R_i(t), x_i(t))$ is bounded for all $i \in \mathcal{V}$.*

Proof. See Appendix A. □

Lemma 10. *For $v_\star$ in Equation (22), there exists an open set $\mathcal{O} \supset v_\star^{-1}(0)$ such that (17) holds for $v = v_\star$.*

Proof. See Appendix A. □

Finally, the solution to Problem 2 is obtained.

Theorem 2. *Consider the system (9) with the control input (15) under a graph G. The desired configuration set $\mathcal{T}((R_i^*, x_i^*)_{i\in\mathcal{V}})$ is*

locally attractive with the relative, distributed controllers (33) having positive constants κ_M and κ_v if and only if G is connected.

Proof. Theorem 1 guarantees that the controllers (15) with (33) for $v = v_\star$ in Equation (22) are reduced to the gradient-based controllers (16). Lemmas 9 and 10 guarantee the assumptions of Lemma 2for $v = v_\star$. Thus, $v_\star^{-1}(0)$ is locally attractive, which is equivalent to $\mathcal{T}((R_i^*, x_i^*)_{i\in\mathcal{V}})$ from Lemma 8 if and only if G is connected. □

4.3 | Properties of the Proposed Method and Comparison to Existing Ones

The proposed controller (33) uses both the orientation discrepancy ${}^*R_j^{[i]}(R_j^{[i]})^\top$ and the position discrepancy $({}^*x_j^{[i]} - \mathrm{avg}(({}^*x_k^{[i]})_{k\in C}))(x_j^{[i]} - \mathrm{avg}((x_k^{[i]})_{k\in C}))^\top$ to determine the orientation control in Equation (28). This structure is unique to this method, ensuring the efficient movement of the agents by restraining drift, which keeps the center of the agent positions stationary and consequently leads to short travel distances. This is justified in Theorem 1. Furthermore, the necessary graph topology is connected, as shown in Theorem 2, which is the same as many existing methods.

Existing controllers do not have such a structure or do not ensure restraining drift, for example, [28] of the form

$$\begin{cases} F_i((R_j^{[i]}, x_j^{[i]}, {}^*R_j^{[i]}, {}^*x_j^{[i]})_{j\in\mathcal{N}_i}) = \alpha_R \sum_{j\in\mathcal{N}_i} \log(R_j^{[i]}({}^*R_j^{[i]})^\top) \\ f_i((R_j^{[i]}, x_j^{[i]}, {}^*R_j^{[i]}, {}^*x_j^{[i]})_{j\in\mathcal{N}_i}) = \alpha_x \sum_{j\in\mathcal{N}_i} (x_j^{[i]} - {}^*x_j^{[i]}) \end{cases} \tag{35}$$

The controller (35) encounters the problems of local minima due to the orientation input. Actually, it is assumed that the initial orientation discrepancy is less than $\pi/2$ for every pair in the literature. Furthermore, (35) determines control input for orientations only from orientation discrepancies $R_j^{[i]}({}^*R_j^{[i]})^\top$ between two agents without consideration of positions. This structure does not restrain the drift, causing unnecessary movement and resulting in longer travel distances while the agents move under unaligned axes. The orientation part of (35) can be replaced to any orientation controllers such as [15, 17]. Reference [15] employs the same structure except for a time-varying graph topology. Reference [17] employs

$$F_i((R_j^{[i]}, x_j^{[i]}, {}^*R_j^{[i]}, {}^*x_j^{[i]})_{j\in\mathcal{N}_i}) = \alpha_R \sum_{j\in\mathcal{N}_i} \dot{f}(\|\log(R_j^{[i]}({}^*R_j^{[i]})^\top)\|) \frac{\log(R_j^{[i]}({}^*R_j^{[i]})^\top)}{\|\log(R_j^{[i]}({}^*R_j^{[i]})^\top)\|} \tag{36}$$

with the reshaping function $f : [0, \pi] \to \mathbb{R}$

$$f(\theta) = \frac{\pi^2 f_0(\theta)}{2 f_0(\pi)} \text{ where } f_0(\theta) = \frac{1}{b} - (\frac{1}{b} - \theta)\exp(-b\theta) \tag{37}$$

which guarantees the almost-global attractiveness of orientations, while the proposed method cannot. However, these methods still involve the issue of the long travel distances.

The primary differences from the authors' previous study [11, 33, 34] are the following two. First, to control the multi-agent system over SE(d) in Equation (9), the control input $(S_i(t), u_i(t))$ must be defined over se(d). Thus, we modified the gradient-based controller from the previous study as (16), where the first equation is newly introduced. Second, as an objective function for the gradient-based controller, we used (22) with (23). Although the form is similar to that in the previous papers, the target set $\mathcal{T}$ was newly designed as (12), which enabled us to treat the orientation and position configurations in a unified way. Then, difficulties arise in the proposed controller (16) with $v = v_\star$ in Equation (22): (i) the convergence to the target set and (ii) whether the controller uses only relative measurements are not guaranteed. The ideas to solve these issues are as follows. (i) First, we showed in Lemma 2 that the convergence to $v^{-1}(0)$ is guaranteed under the additional condition (17). Therefore, we determined the proposed function $v_\star$ in Equation (22) to satisfy (17) in Lemma 10, where the characteristics of SE(d) are crucial to prove the lemma in Appendix A. Finally, the convergence to a desired configuration was ensured in Theorem 2. (ii) The key property of the gradient of v_C in Equation (23) is the linearity in R_i and the invariance in x_i, R_i^*, and x_i^*, as shown in Lemma 6, that is, (31) and (32). The proof of this lemma relies on the properties of SE(d) as shown in Appendix A. By using Equations (31) and (32), the controller is ensured to use only relative measurements and relative desired poses, as shown in Theorem 1. Furthermore, the stationary center (14) of the agents is guaranteed.

5 | Numerical Experiments

5.1 | Case of 2-D Space for 7 Agents

In this section, simulations in 2-D space are provided to verify the effectiveness of the proposed method by comparison with other methods. A system composed of 7 agents is considered with the sensing graph G, of which the edges are presented in Figure 4, which has a cycle. The desired poses are shown in Figure 4. Each agent is modeled using Equation (9).

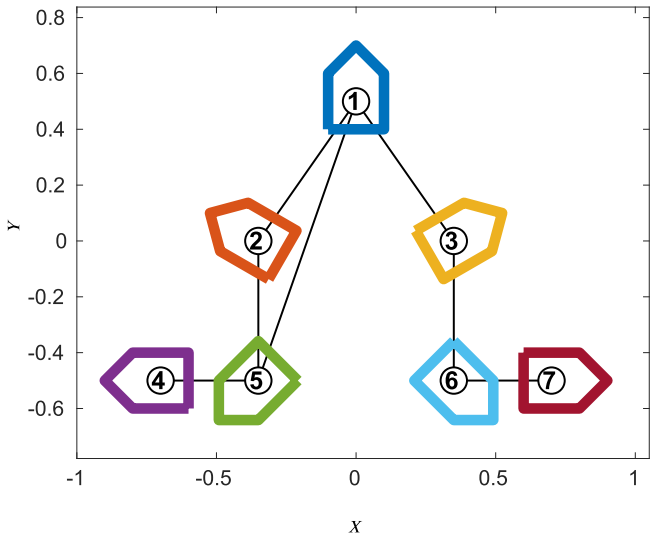

FIGURE 4 | Desired poses in 2-D space.

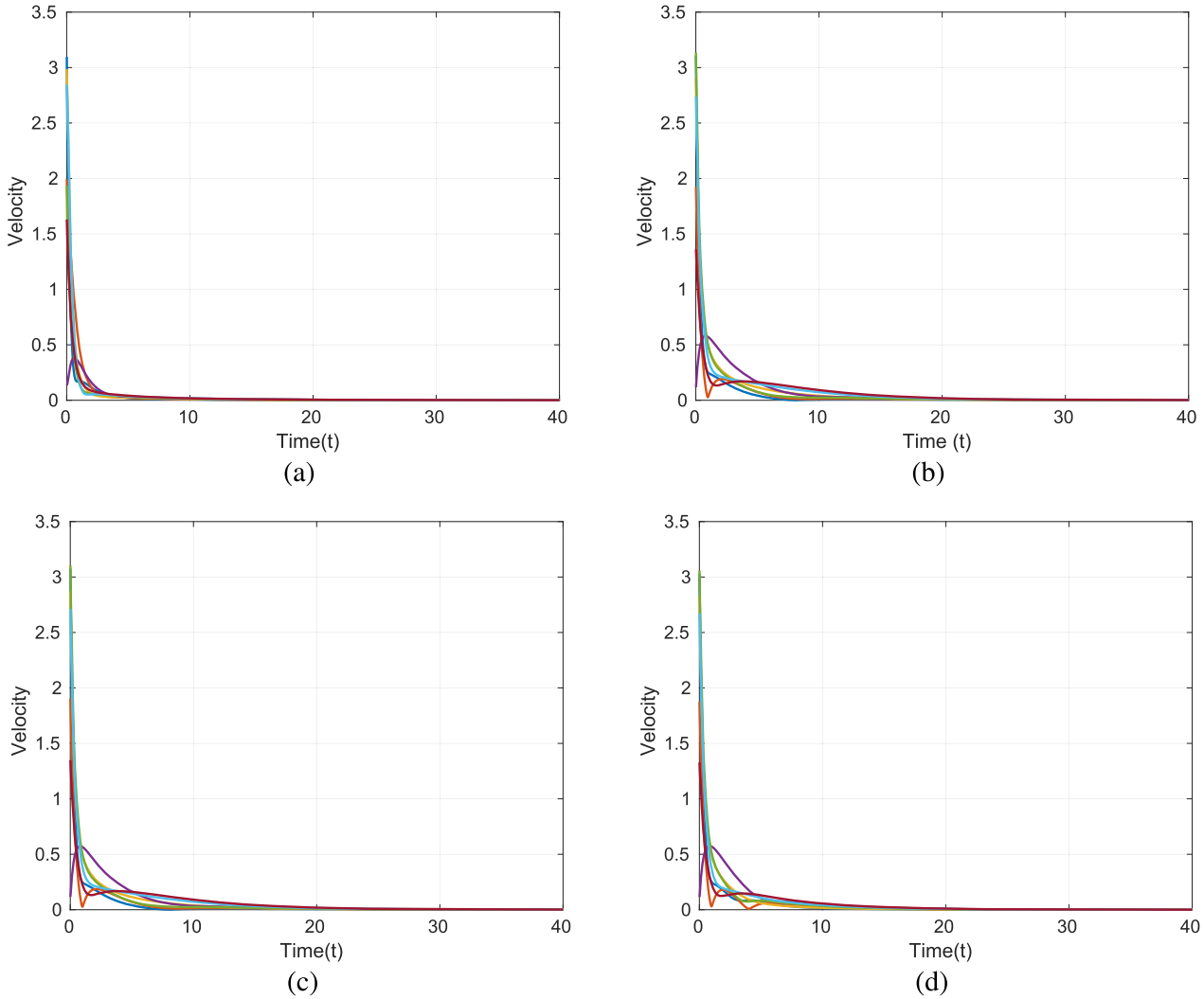

FIGURE 5 | Velocities with (a) the proposed method, those of (b) Reference [28], (c) Reference [15], and (d) Reference [17].

We employ (a) the proposed controller (33) with gains $\kappa_M = 0.158$ and $\kappa_v = 1.84$, (b) the controller (35) of [28] with $\alpha_R = 0.0735$ and $\alpha_x = 0.679$, (c) the controller (35) of [15] with $\alpha_R = 0.0741$ and $\alpha_x = 0.672$, and (d) the controller (36) and (37) of [17] with $\alpha_R = 0.0603$, $b = 1.0$, and $\alpha_x = 0.662$. Because [15, 17] offer only orientation controllers, the position controller of [28] is used. The gains of these controllers are set to have similar local convergence characteristics of velocities and angular velocities, as shown in Figures 5–7, which depict the velocities $\|\dot{x}_i(t)\|$, angular velocities $\|\dot{R}_i(t)\|$, and trajectories $x_i(t)$, respectively, from the same initial poses. The desired poses in Figure 4 are achieved by all controllers.

We conduct simulations from 100 random initial poses for each controller with the sampling time of 0.01. Table 1 shows the success rates in simulations with the averages and maximums of the travel distances of the center of the agent positions, $\|\sum_{i=1}^{7}(x_i(200) - x_i(0))/n\|$, when the formation is successfully achieved. The success rates with (a) the proposed method and (d) the method of [17] are 100% while those of (b) and (c) are 76%. Note that the success rates of (b) and (c) are low, basically due to the cycle in the graph, while (a) the proposed method is not deteriorated by the cycle. On the other hand, the travel distances of the center of the agent positions of (a) the proposed method are always zero, while those of (b)–(d) the other methods are more than 1.64 on average and 7.06 on maximum, which leads to the drift of the agents. The typical trajectories from the same initial poses are depicted in Figure 8. These figures show that the agents travel significantly shorter distances with (a) the proposed method than (b)–(d) the other methods. These results indicate the advantages of the proposed method.

5.2 | Case of 2-D Space for 22 Agents

In this section, simulation results in 2-D space for 22 agents are provided. The sensing graph G and desired poses are shown in Figure 9. The simulation setting is the same as the case of 7 agents, except for the agent number, the sensing network, and the desired formation. The simulation results from 100 random initial poses are shown in Table 2. The success rates of (a) the proposed method and (d) the existing method are 100%, while those of (b) and (c) are only 13%, which shows that methods (b)

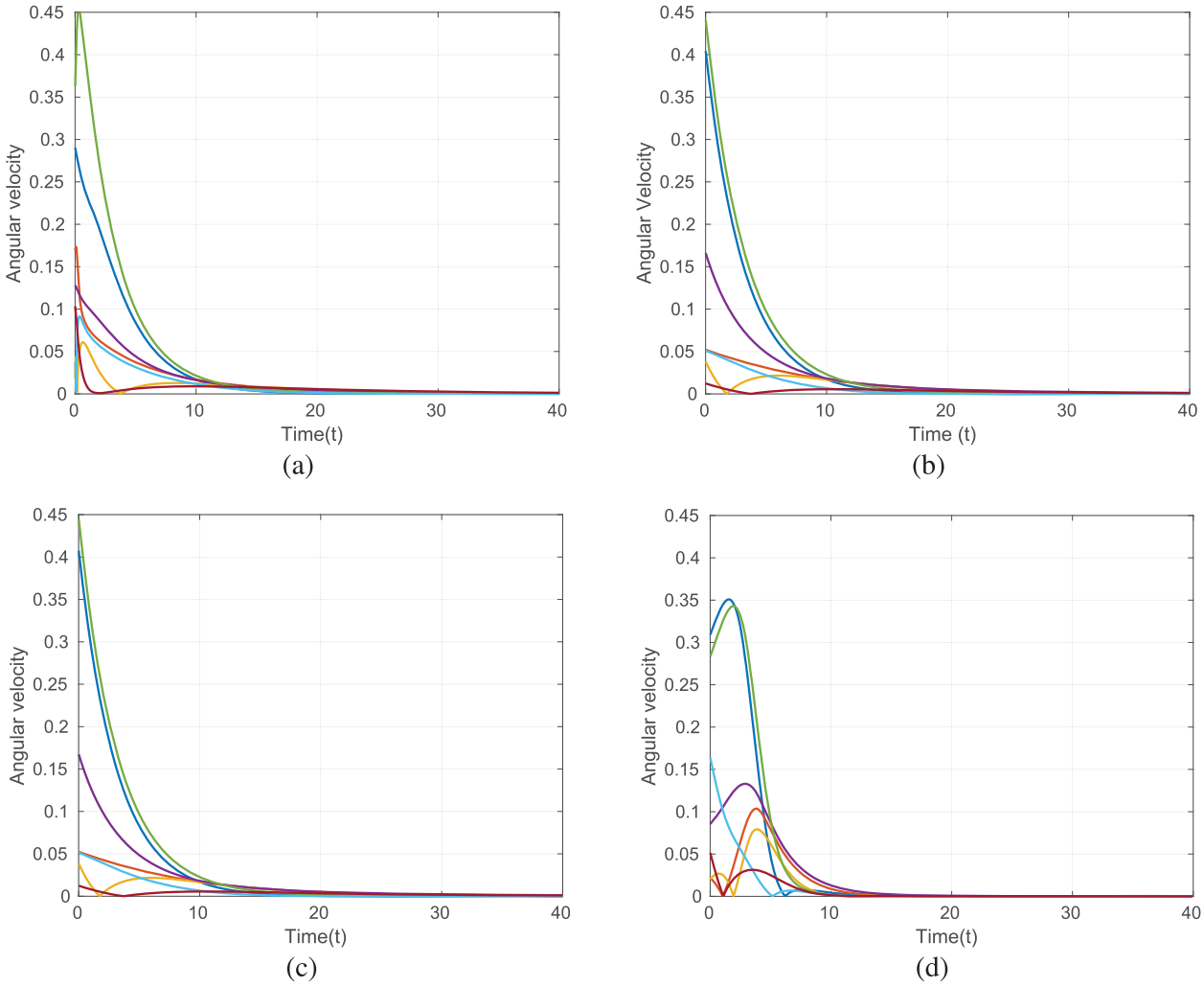

FIGURE 6 | Angular velocities with (a) the proposed method, those of (b) Reference [28], (c) Reference [15], and (d) Reference [17].

and (c) significantly decrease the success rate as the number of agents increases, while the proposed method and (d) do not. Furthermore, the travel distances of the center of the agent positions in (a) the proposed method are always zero, while those of the other methods are not. The typical trajectories from the same initial poses are depicted in Figure 10, which show the shorter travel distances with (a) the proposed method than (b)–(d) the other methods. These results indicate the advantages of the proposed method regardless of the agent number.

5.3 | Case of 2-D Space for 100 Agents

In this section, a simulation result in 2-D space for 100 agents is provided. The sensing graph G and desired poses are shown in Figure 11a. The simulation result with the proposed method is depicted in Figure 11b, which shows that the desired poses are achieved. This result indicates the scalability of the proposed method.

5.4 | Case of 3-D Space

We conduct a simulation in 3-D space to verify the effectiveness of the proposed method regardless of the dimension of space. The sensing graph and the desired configuration are shown in Figure 12a. Figure 12b–d provide a snapshot of the simulation process, which shows that the agents achieve the desired configuration with some rotation and translation. Thus, the proposed method is applicable to any dimensional space.

6 | Conclusion

This study proposed a method for the distributed SE(d) formation control of multiple agents using only relative measurements. The clique-based distributed pattern matching technique was improved to address both formation and orientation control, and a distributed and a relative controller was developed to evaluate the discrepancy between the agents' current and desired poses.

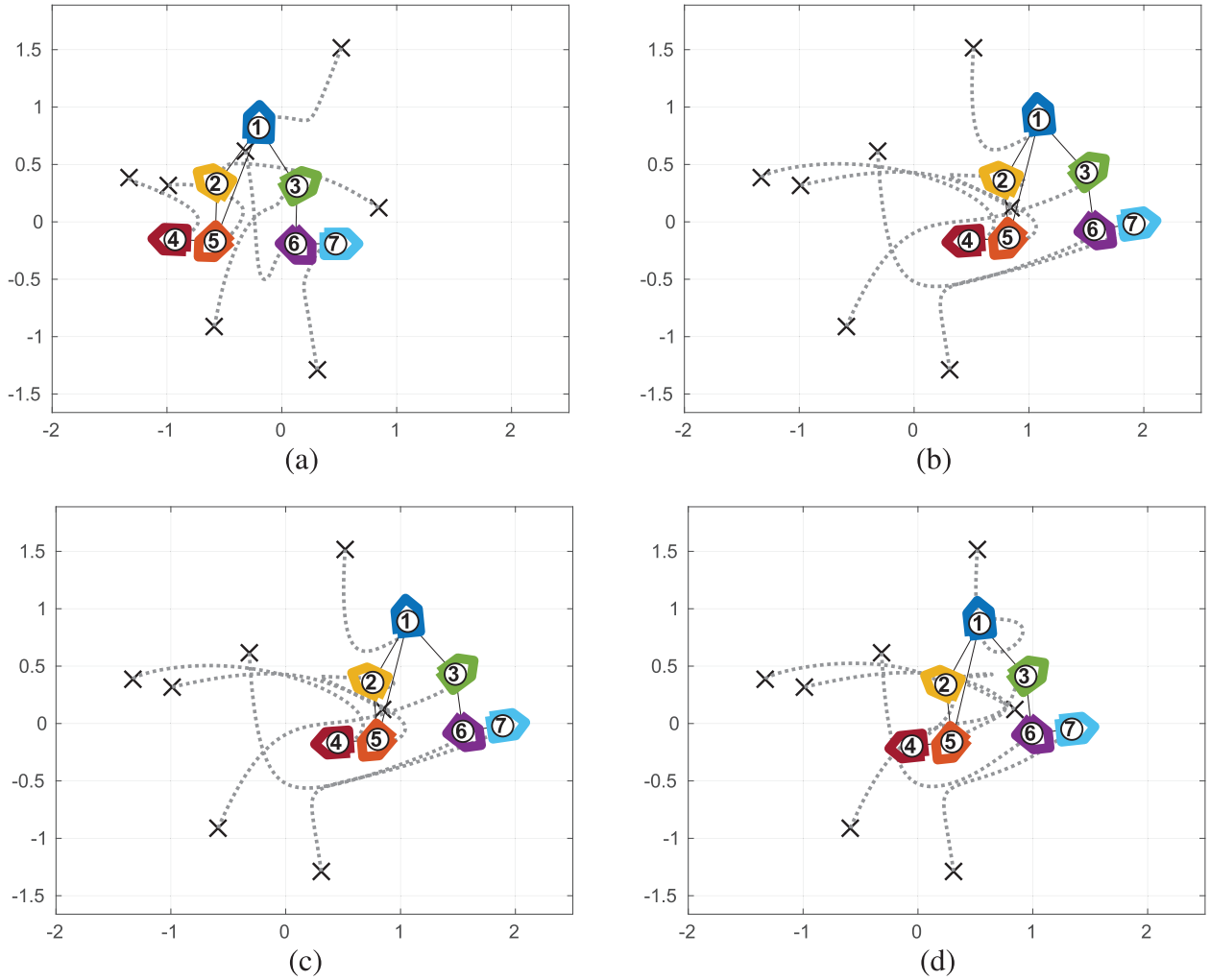

FIGURE 7 | Trajectories with (a) the proposed method, those with (b) Reference [28], (c) Reference [15], and (d) Reference [17].

TABLE 1 | Success rate, average, and maximum of the travel distances of the center of agent positions.

Controller	Success rate	Dist. average	Dist. maximum
(a) Proposed	100%	0.0	0.0
(b) [28]	76%	13.9	176
(c) [15]	76%	13.7	174
(d) [17]	100%	1.64	7.06

Moreover, the desired configuration of the system was proven to be attractive. Simulation results demonstrated the effectiveness of the proposed controller in both 2-D and 3-D space cases. The results of this study raise a number of open issues, such as considering non-holonomic constraints on the kinematic model of agents. Although we proved only a local attraction, the simulation result shows the large attraction region provided by the proposed method. Our future work includes the evaluation of the attraction region and the design of a distributed pose controller over a time-varying digraph, which may lead to a more relaxed condition as a joint graph containing a spanning tree. We assume that the agents can measure their neighbors' relative poses. However, the relative pose is sometimes difficult to measure accurately by camera or LiDAR. Even in such a case, the distance or bearing of neighbors is possibly available. On the other hand, the absolute position or pose may be available by using GNSS or SLAM, and other information can be exchanged if network communication is available. This article does not deal with such cases of less/more information. To adapt the proposed method to less/more information, we may modify the control objective from Equation (10) to a suitable one according to the available information, which is crucial future work. The further challenge is to bridge the theory-practice gap, such as robust sensing (fusing multiple sensing modalities and applying outlier rejection algorithms to refine relative pose estimation) and hardware-aware control (implementing low-pass filtering or predictive control to offset actuator delays and adapt to dynamic constraints).

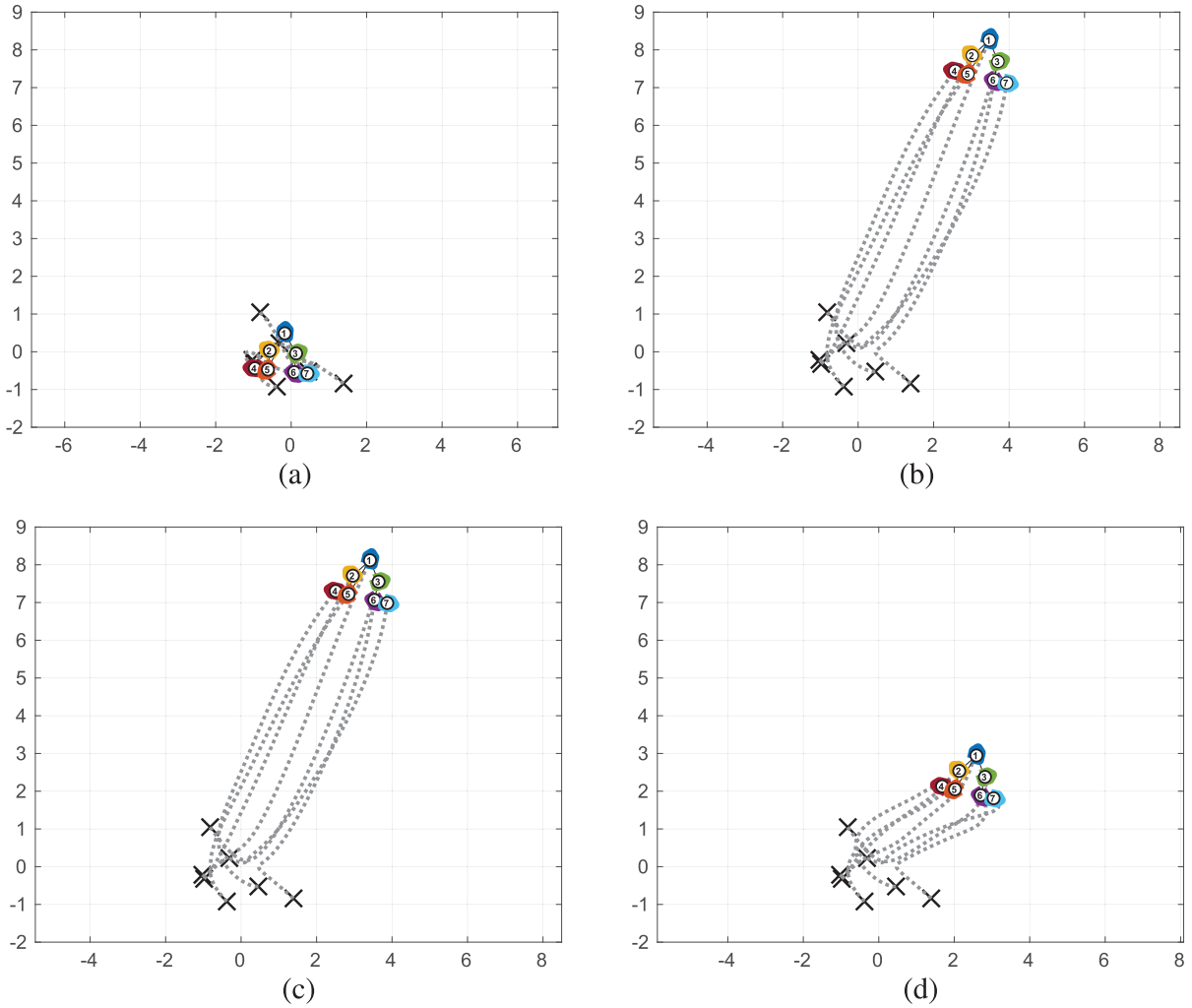

FIGURE 8 | Trajectories from different initial poses with (a) the proposed method, those with (b) Vision-Based Distributed Formation Control Without an External Positioning System, (c) Distributed attitude synchronization control of multi-agent systems with switching topologies, and (d) Intrinsic Consensus on SO(3) with Almost-Global Convergence.

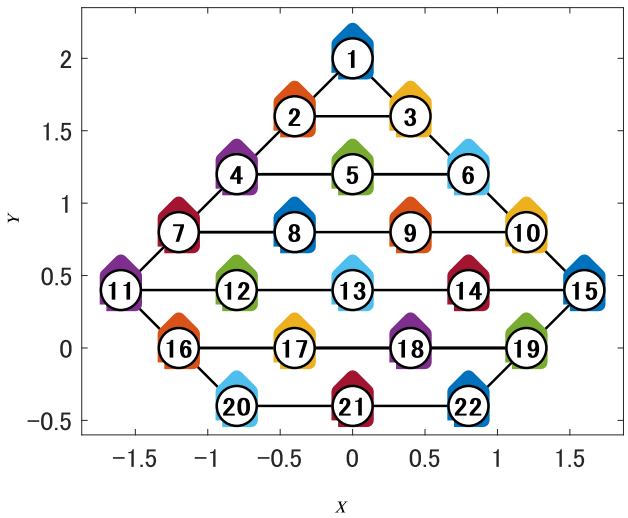

FIGURE 9 | Desired poses in 2-D space for 22 agents.

TABLE 2 | Success rate, average, and maximum of the travel distances of the center of agent positions for 22 agents.

Controller	Success rate	Dist. average	Dist. maximum
(a) Proposed	100%	0.0	0.0
(b) [28]	13%	63.7	173
(c) [15]	13%	63.2	171
(d) [17]	100%	1.84	12.4

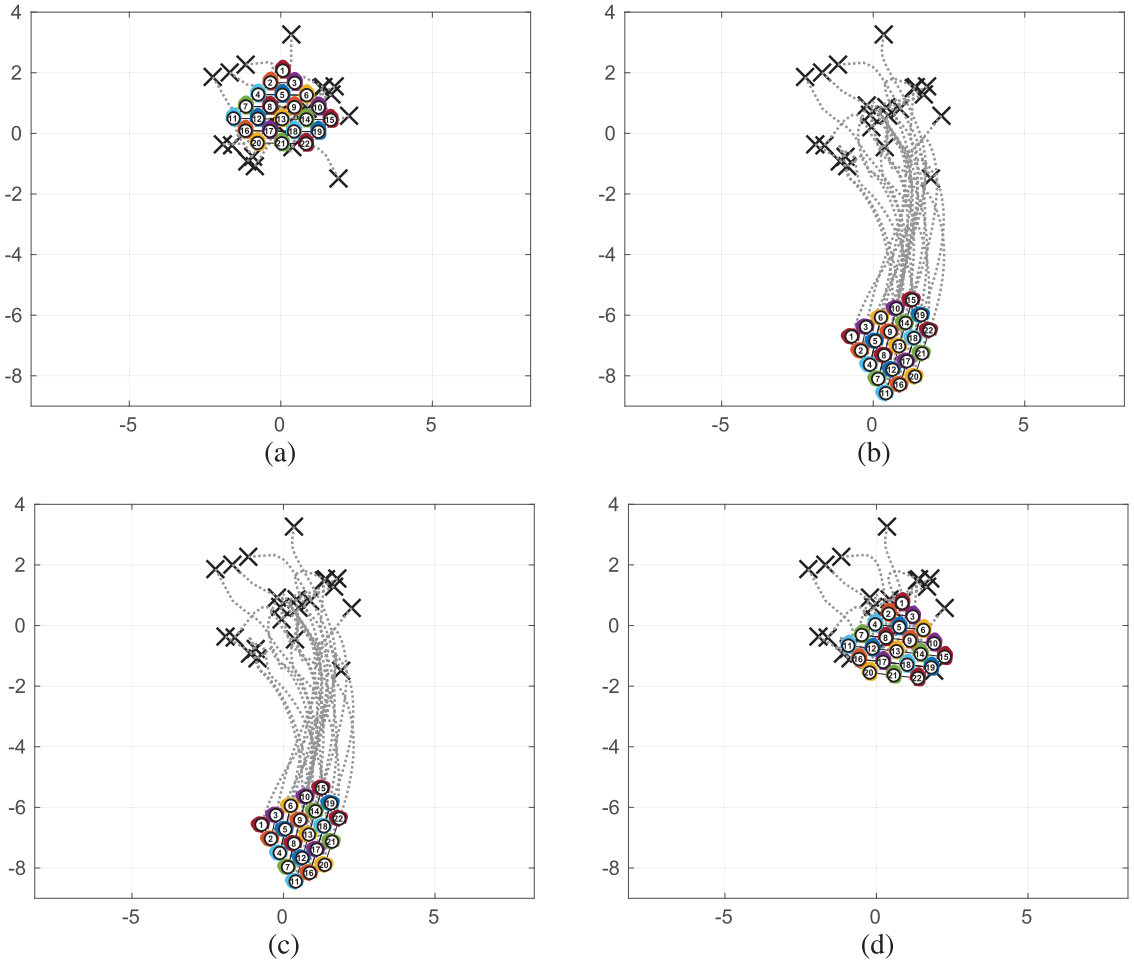

FIGURE 10 | Trajectories from different initial poses with (a) the proposed method, those with (b) Reference [28], (c) Reference [15], and (d) Reference [17] for 22 agents.

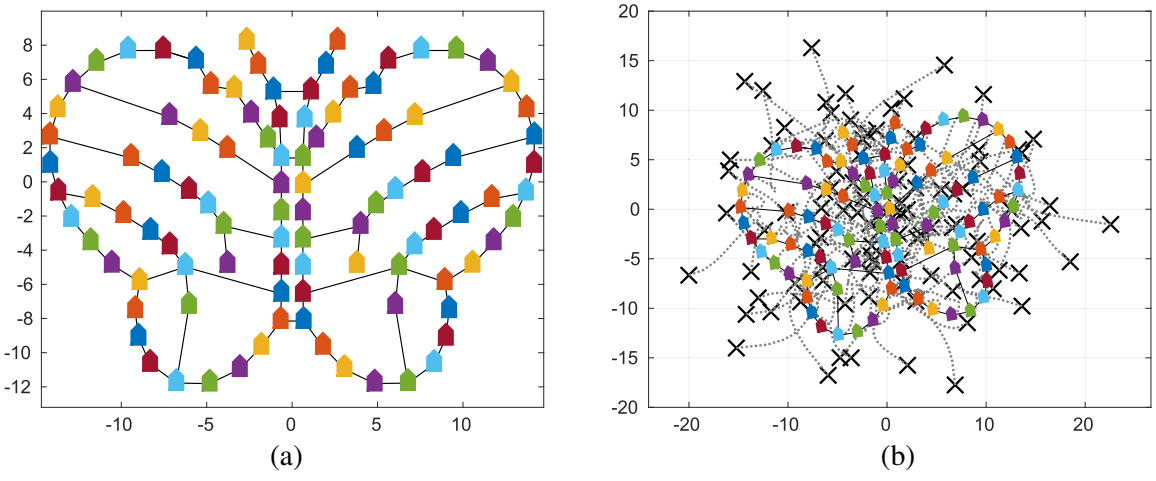

FIGURE 11 | (a) Desired poses in 2-D space for 100 agents, (b) trajectories with the proposed method.

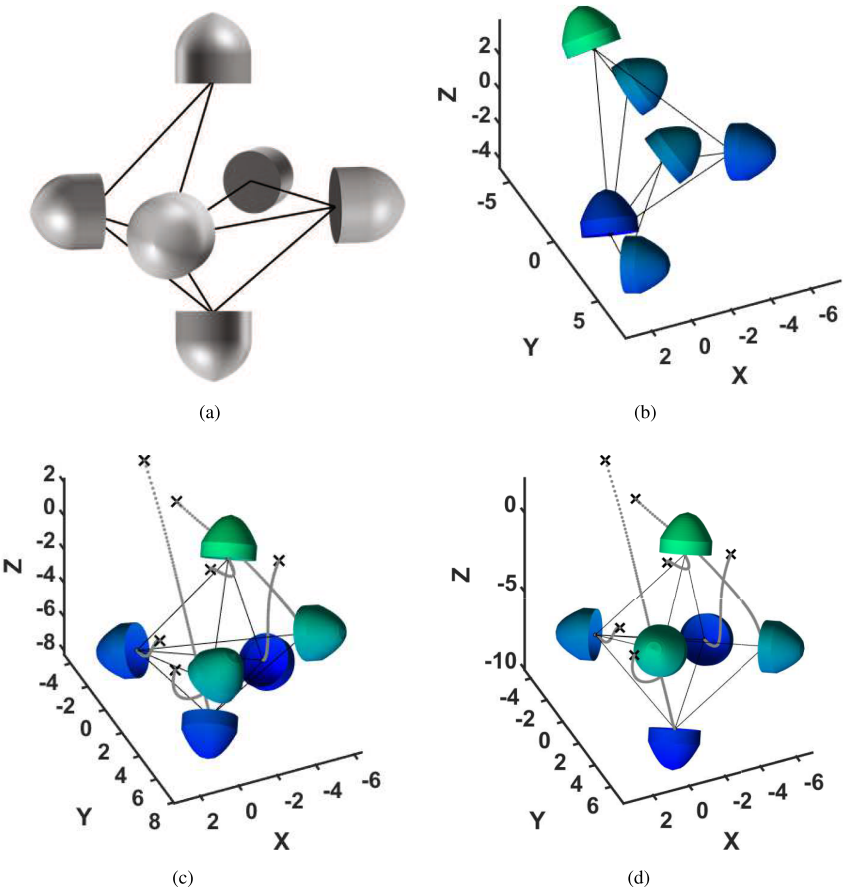

FIGURE 12 | Simulation result in 3-D space. (a) Desired configuration, (b) $t = 0$, (c) $t = 10$, and (d) $t = 25$.

Conflicts of Interest

The authors declare no conflicts of interest.

Data Availability Statement

The data that support the findings of this study are available from the corresponding author upon reasonable request.

References

1. R. Tron, J. Thomas, G. Loianno, K. Daniilidis, and V. Kumar, "A Distributed Optimization Framework for Localization and Formation Control: Applications to Vision-Based Measurements," *IEEE Control Systems Magazine* 36, no. 4 (2016): 22–44.

2. C. Peng and T. Wang, "An Improved Energy-Aware and Self-Adaptive Deployment Method for Autonomous Underwater Vehicles," *International Journal of Modelling, Identification and Control* 31, no. 2 (2019): 182–192.

3. S. Zhao and D. Zelazo, "Translational and Scaling Formation Maneuver Control via a Bearing-Based Approach," *IEEE Transactions on Control of Network Systems* 4, no. 3 (2015): 429–438.

4. S. Coogan and M. Arcak, "Scaling the Size of a Formation Using Relative Position Feedback," *Automatica* 48, no. 10 (2012): 2677–2685.

5. Z. Meng, B. D. Anderson, and S. Hirche, "Formation Control With Mismatched Compasses," *Automatica* 69 (2016): 232–241.

6. K. K. Oh, M. C. Park, and H. S. Ahn, "A Survey of Multi-Agent Formation Control," *Automatica* 53 (2015): 424–440.

7. L. Krick, M. E. Broucke, and B. A. Francis, "Stabilisation of Infinitesimally Rigid Formations of Multi-Robot Networks," *International Journal of Control* 3 (2009): 423–439.

8. X. Cai and M. d. Queiroz, "Rigidity-Based Stabilization of Multi-Agent Formations," *Journal of Dynamic Systems, Measurement, and Control* 136, no. 1 (2014): 014502.

9. B. D. O. Anderson, Z. Sun, T. Sugie, S. Azuma, and K. Sakurama, "Formation Shape Control With Distance, and Area Constraints," *IFAC Journal of Systems and Control* 1, no. 8 (2017): 2–12.

10. K. Sakurama, S. Azuma, and T. Sugie, "Distributed Controllers for Multi-Agent Coordination via Gradient-Flow Approach," *IEEE Transactions on Automatic Control* 60, no. 6 (2015): 1471–1485.

11. K. Sakurama, S. Azuma, and T. Sugie, "Multiagent Coordination via Distributed Pattern Matching," *IEEE Transactions on Automatic Control* 64, no. 8 (2019): 3210–3225.

12. G. Krieger, H. Fiedler, and A. Moreira, "Earth Observation With SAR Satellite Formations: New Techniques and Innovative Products," in *Proceedings of the IAA Symp. On Small Satellites for Earth Observation* (IAA, 2009).

13. J. Xiong, J. W. Cheong, Z. Xiong, A. G. Dempster, S. Tian, and R. Wang, "Integrity for Multi-Sensor Cooperative Positioning," *IEEE Intelligent Transportation Systems Magazine* 22, no. 2 (2021): 792–807.

14. J. Thunberg, E. Montijano, and X. Hu, "Distributed Attitude Synchronization Control," in *Proceedings of the 50th IEEE Conference on Decis. Control. And Eur Control. Conf* (IEEE, 2011), 1962–1967.

15. J. Thunberg, W. Song, E. Montijano, Y. Hong, and X. Hu, "Distributed Attitude Synchronization Control of Multi-Agent Systems With Switching Topologies," *Automatica* 50, no. 3 (2014): 832–840.

16. Y. Igarashi, T. Hatanaka, M. Fujita, and M. W. Spong, "Passivity-Based Attitude Synchronization in SE(3)," *IEEE Transactions on Control Systems Technology* 17, no. 5 (2009): 1119–1134.

17. R. Tron, B. Afsari, and R. Vida, "Intrinsic Consensus on SO(3) With Almost-Global Convergence," in *Proceedings of the 51st IEEE Conference on Decis. Control. And Eur Control. Conf* (IEEE, 2012), 2052–2058.

18. W. Song, Y. Tang, Y. Hong, and X. Hu, "Relative Attitude Formation Control of Multi-Agent Systems," *International Journal of Robust and Nonlinear Control* 27 (2017): 4457–4477.

19. B. H. Lee, S. M. Kang, and H. S. Ahn, "Distributed Orientation Estimation in SO(d) and Applications to Formation Control and Network Localization," *IEEE Transactions on Control of Network Systems* 6, no. 4 (2018): 1302–1312.

20. Q. V. Tran and H. S. Ahn, "Distributed Formation Control of Mobile Agents via Global Orientation Estimation," *IEEE Transactions on Control of Network Systems* 7, no. 4 (2020): 1654–1664.

21. J. G. Lee, M. H. Trinh, H. S. Ahn, and B. H. Lee, "Distributed Formation Control of the Special Euclidean Group SE(2) via Global Orientation Control," *IET Control Theory and Applications* 14, no. 10 (2020): 1393–1399.

22. K. Oh and H. Ahn, "Formation Control of Rigid Bodies Based on Orientation Alignment and Position Estimation," in *Proceedings of 2014 14th International Conference on Control., Automation and Syst* (ICROS, 2014), 740–744.

23. C. K. Verginis, A. Nikou, and D. V. Dimarogonas, "Robust Formation Control in for Tree-Graph Structures With Prescribed Transient and Steady State Performance," *Automatica* 103 (2019): 538–548.

24. H. Niu and Z. Geng, "Almost-Global Formation Tracking Control for Multiple Vehicles With Disturbance Rejection," *IEEE Access* 6 (2018): 25632–25645.

25. X. Peng, J. Sun, and Z. Geng, "The Geometric Convexity on SE(3) and Its Application to the Formation Tracking in Multi-Vehicle Systems," *International Journal of Control* 92, no. 3 (2019): 528–539.

26. K. K. Oh and H. S. Ahn, "Formation Control and Network Localization via Orientation Alignment," *IEEE Transactions on Automatic Control* 59, no. 2 (2013): 540–545.

27. J. Thunberg, J. Goncalves, and X. Hu, "Consensus and Formation Control on SE(3) for Switching Topologies," *Automatica* 66 (2016): 109–121.

28. E. Montijano, E. Cristofalo, D. Zhou, M. Schwager, and C. Sagüés, "Vision-Based Distributed Formation Control Without an External Positioning System," *IEEE Transactions on Robotics* 32, no. 2 (2016): 339–351.

29. M. Nazari, E. A. Butcher, T. Yucelen, and A. K. Sanyal, "Decentralized Consensus Control of a Rigid-Body Spacecraft Formation With Communication Delay," *Journal of Guidance, Control, and Dynamics* 39, no. 4 (2016): 838–851.

30. L. Chen, M. Cao, and C. Li, "Bearing Rigidity and Formation Stabilization for Multiple Rigid Bodies in SE(3)," *Numerical Algebra, Control and Optimization* 9, no. 3 (2019): 257–267.

31. B. Pozzan, G. Michieletto, A. Cenedese, and D. Zelazo, "Heterogeneous Formation Control: A Bearing Rigidity Approach," in *Proceedings of the 60st IEEE Conference on Decis. Control* (IEEE, 2021), 6451–6456.

32. C. Peng and K. Sakurama, "Distributed Formation and Orientation Control of Multiple Holonomic Mobile Robots Using Relative Measurements," in *Proceedings of the 5th IEEE Conference on Control Technology and Applications* (IEEE, 2021).

33. K. Sakurama, "Unified Formulation of Multi-Agent Coordination With Relative Measurements," *IEEE Transactions on Automatic Control* 66, no. 9 (2021): 4101–4116.

34. K. Sakurama and T. Sugie, "Generalized Coordination of Multi-Robot Systems," *Foundations and Trends in Systems and Control* 9, no. 1 (2021): 1–170.

35. K. Kanatani, "Analysis of 3-D Rotation Fitting," *IEEE Transactions on Pattern Analysis and Machine Intelligence* 16, no. 5 (1994): 543–549.

36. F. Bullo and A. D. Lewis, "Geometric Control of Mechanical Systems: Modeling," in *Analysis, and Design for Simple Mechanical Control Systems* (Springer Science+Business Media, 2004).

37. H. K. Khalil, *Nonlinear Systems* (Prentice Hall, 2002).

38. J. Nash, "Real Algebraic Manifolds," *Annals of Mathematics* 56 (1952): 405–421.

39. M. P. Denkowski, "On the Points Realizing the Distance to a Definable Set," *Journal of Mathematical Analysis and Applications* 378 (2011): 592–602.

40. S. Lojasiewicz, *Ensembles Semi-Analytiques* (Institut des Hautes Etudes Scientifiques, 1965).

41. S. Lojasiewicz and M. Zurro, "On the Gradient Inequality," *Bulletin of the Polish Academy of Sciences-Mathematics* 47, no. 2 (1965): 143–145.

42. F. Rupp, "On the Lojasiewicz-Simon Gradient Inequality on Submanifolds," *Journal of Functional Analysis* 279 (2020): 108708.

Appendix A

Proofs of Lemmas

Proof of Lemma 2

From the property of the projection (1) such that $\langle X, \mathcal{P}_{\mathrm{skew}}(X)\rangle = \|\mathcal{P}_{\mathrm{skew}}(X)\|^2$, the time-derivative of the function v in Equation (16) for the differential equation (9) is calculated as

$$\begin{aligned}\frac{dv}{dt} &= \sum_{i=1}^{n}\left(\langle \frac{\partial v}{\partial x_i}, \dot{x_i}\rangle + \langle \frac{\partial v}{\partial R_i}, \dot{R_i}\rangle\right)\\ &= -\sum_{i=1}^{n}\left(\left\|\frac{\partial v}{\partial x_i}\right\|^2 + \langle R_i^\top \frac{\partial v}{\partial R_i}, \mathcal{P}_{\mathrm{skew}}\left(R_i^\top \frac{\partial v}{\partial R_i}\right)\rangle\right)\\ &= -\sum_{i=1}^{n}\left(\left\|\frac{\partial v}{\partial x_i}\right\|^2 + \left\|\mathcal{P}_{\mathrm{skew}}\left(R_i^\top \frac{\partial v}{\partial R_i}\right)\right\|^2\right) \le 0 \end{aligned} \tag{A1}$$

For a constant $\epsilon > 0$, let $\mathcal{L}_\epsilon = \bigcup_{0\le c\le \epsilon} v^{-1}(c)$ denote the sub-level set of v, and let $\mathring{\mathcal{L}}_\epsilon$ denote the interior of $\mathcal{L}_\epsilon$. From Equation (A1), for $(R_i(0), x_i(0))_{i\in\mathcal{V}} \in \mathring{\mathcal{L}}_\epsilon$, $(R_i(t), x_i(t))_{i\in\mathcal{V}} \in \mathring{\mathcal{L}}_\epsilon$ holds for any $t \ge 0$. From the assumption of the boundedness of $(R_i(t), x_i(t))_{i\in\mathcal{V}}$, for each $(R_i(0), x_i(0))_{i\in\mathcal{V}}$, there is an open bounded set $\mathcal{R}((R_i(0), x_i(0))_{i\in\mathcal{V}})$ such that $(R_i(t), x_i(t))_{i\in\mathcal{V}} \in \mathcal{R}((R_i(0), x_i(0))_{i\in\mathcal{V}})$ for any t. For each $(\tilde{R}_i, \tilde{x}_i)_{i\in\mathcal{V}} \in \partial(v^{-1}(0))$, where $\partial(v^{-1}(0))$ denotes the boundary of $v^{-1}(0)$, set a function $\epsilon((\tilde{R}_i, \tilde{x}_i)_{i\in\mathcal{V}}) > 0$ and an open bounded set $\mathcal{S}((\tilde{R}_i, \tilde{x}_i)_{i\in\mathcal{V}}) \subset \mathring{\mathcal{L}}_{\epsilon((\tilde{R}_i,\tilde{x}_i)_{i\in\mathcal{V}})}$ to satisfy $\mathring{\mathcal{L}}_{\epsilon((\tilde{R}_i,\tilde{x}_i)_{i\in\mathcal{V}})} \cap (\bigcup_{(\hat{R}_i,\hat{x}_i)_{i\in\mathcal{V}}\in\mathcal{S}((\tilde{R}_i,\tilde{x}_i)_{i\in\mathcal{V}})} \mathcal{R}((\hat{R}_i, \hat{x}_i)_{i\in\mathcal{V}}) \subset \mathcal{O}$, which is possible because $\mathcal{O}$ is an open set containing $v^{-1}(0)$ satisfying (17). Then, for any initial state $(R_i(0), x_i(0))_{i\in\mathcal{V}} \in \mathcal{S}((\tilde{R}_i, \tilde{x}_i)_{i\in\mathcal{V}})$, $(R_i(t), x_i(t))_{i\in\mathcal{V}} \in \mathcal{O}$ holds. From Equation (A1), LaSalles' invariance principle [37] guarantees that

$$\lim_{t\to\infty} \mathrm{dist}((R_i(t), x_i(t))_{i\in\mathcal{V}}, \mathcal{Q}) = 0 \tag{A2}$$

where $\mathcal{Q} \subset (\mathrm{SE}(d))^n$ is the largest invariant set contained in $((\mathcal{P}_{\mathrm{skew}}(R_i^\top \frac{\partial v}{\partial R_i}), \frac{\partial v}{\partial x_i})_{i\in\mathcal{V}})^{-1}(0)$. Therefore, the solution converges to a point

in the set $\mathcal{Q} \cap \mathcal{O}$. This set is contained in $((\mathcal{P}_{\text{skew}}(R_i^\top \frac{\partial v}{\partial R_i}), \frac{\partial v}{\partial x_i})_{i\in\mathcal{V}})^{-1}(0) \cap \mathcal{O}$, and from Equation (17), the solution converges to $v^{-1}(0)$. This holds for any initial state $(R_i(0), x_i(0))_{i\in\mathcal{V}}$ in $\bigcup_{(\bar{R}_i,\bar{x}_i)_{i\in\mathcal{V}}\in\partial(v^{-1}(0))} \mathcal{S}((\bar{R}_i,\bar{x}_i)_{i\in\mathcal{V}}) \cup \mathring{v}^{-1}(0)$, which is an open set containing $v^{-1}(0)$. Thus, $v^{-1}(0)$ is locally attractive.

Proof of Lemma 4

The solution of $\hat{\tau}_C$ in Equation (26) has the same structure of $\hat{\tau}$ given in Equation (7), that is, (27), with which the optimization problem in Equation (26) is reduced to

$$\begin{aligned}\min_{\hat{R}_C\in\mathrm{SO}(d)} \sum_{j\in C}(\kappa_M(\|R_j\|^2 + \|R_j^*\|^2) - 2\mathrm{tr}\Bigg(\hat{R}_C^\top \sum_{j\in C}(\kappa_M R_j^* R_j^\top \\ +\kappa_v(x_j^* - \mathrm{avg}((x_k^*)_{k\in C}))(x_j - \mathrm{avg}((x_k)_{k\in C}))^\top)\Bigg) \\ + \kappa_v(\|x_j^* - \mathrm{avg}((x_k^*)_{k\in C})\|^2) + \|x_j - \mathrm{avg}((x_k)_{k\in C})\|^2)) \end{aligned} \tag{A3}$$

Equation (5) is reduced to

$$\min_{\hat{R}\in\mathrm{SO}(d)} \sum_{j=1}^n (\|x_j\|^2 + \|x_j^*\|^2) - 2\mathrm{tr}(\hat{R}^\top \sum_{j=1}^n x_j x_j^{*\top}) \tag{A4}$$

Compare (A3) and (A4), and from Equations (6) and (7), the solution to the optimization problem (26) is given by $(\hat{R}_C.\hat{\tau}_C)$ in Equaitons (27) and (28).

Proof of Lemma 5

With $(\hat{R}_C, \hat{\tau}_C)$ given in Equation (27), (26) is reduced to

$$\begin{aligned}&\hat{v}_C((R_j, x_j, R_j^*, x_j^*)_{j\in C}) \\ &= \sum_{j\in C}\frac{1}{2}(\kappa_M\|R_j - \hat{R}_C R_j^*\|^2 + \kappa_v\|x_j - \mathrm{avg}((x_k)_{k\in C}) \\ &\quad - \hat{R}_C(x_j^* - \mathrm{avg}((x_k^*)_{k\in C}))\|^2) \\ &= \sum_{j\in C}\frac{1}{2}(\kappa_M(\|R_j\|^2 + \|\hat{R}_C R_j^*\|^2) - 2\mathrm{tr}(\hat{R}_C(\kappa_M R_j^* R_j^\top \\ &\quad + \kappa_v(x_j^* - \mathrm{avg}((x_k^*)_{k\in C}))(x_j - \mathrm{avg}((x_k)_{k\in C}))^\top)) \\ &\quad + \kappa_v(\|x_j - \mathrm{avg}((x_k)_{k\in C})\|^2 + \|\hat{R}_C(x_j^* - \mathrm{avg}((x_k^*)_{k\in C}))\|^2))\end{aligned}$$

Since $\hat{R}_C \in \mathrm{SE}(d)$ for any R_i, the partial derivative of $\hat{v}_C$ with respect to R_i is achieved as

$$\begin{aligned}\frac{\partial \hat{v}_C}{\partial R_i} = \frac{\kappa_M}{2}\frac{\partial\|R_i\|^2}{\partial R_i} - \sum_{j\in C}\frac{\partial}{\partial R_i}\mathrm{tr}(\hat{R}_C(\kappa_M R_j^* R_j^\top \\ + \kappa_v(x_j^* - \mathrm{avg}((x_k^*)_{k\in C}))(x_j - \mathrm{avg}((x_k)_{k\in C}))^\top))\end{aligned} \tag{A5}$$

The (l, m) entry of the term in the sum in Equation (A5) is reduced to

$$\begin{aligned}\kappa_M\mathrm{tr}\left(\hat{R}_C\frac{\partial(R_i^* R_i^\top)}{\partial[R_i]_{lm}}\right) + \sum_{j\in C}\mathrm{tr}\Bigg(\frac{\partial\hat{R}_C}{\partial[R_i]_{lm}}(\kappa_M R_j^* R_j^\top \\ +\kappa_v(x_j^* - \mathrm{avg}((x_k^*)_{k\in C}))(x_j - \mathrm{avg}((x_k)_{k\in C}))^\top)\Bigg)\end{aligned} \tag{A6}$$

where the (l, m) entry of a matrix R is denoted as $[R]_{lm}$. The first term in Equation (A6) is reduced to

$$\mathrm{tr}\left(\hat{R}_C\frac{\partial(R_i^* R_i^\top)}{\partial[R_i]_{lm}}\right) = \mathrm{tr}\left(\hat{R}_C R_i^*\frac{\partial R_i^\top}{\partial[R_i]_{lm}}\right) = e_{dl}^\top \hat{R}_C R_i^* e_{(dn)m} \tag{A7}$$

where $e_{dl} \in \mathbb{R}^d$ denotes the d-dimensional unit vector whose l-th component is 1. The second term in Equation (A6) can be shown to be zero from the same calculation as [11]. From this, (A5), (A6), and (A7), (29) is obtained. (30) can be derived in the same way.

Proof of Lemma 6

Let $(Z_j, y_j) = R(R_j, x_j + \tau)$ and $(Z_j^*, y_j^*) = R^*(R_j^*, x_j^* + \tau^*)$, and let $\overline{R}_C$ be the matrix satisfying (27) for (Z_j, y_j) and (Z_j^*, y_j^*) instead of (R_j, x_j) and (R_j^*, x_j^*). From Equations (27) and (28), the following equations hold:

$$\overline{R}_C = \overline{V}\mathrm{diag}(1, \ldots, 1, \det(\overline{V}\bar{U}^\top))\bar{U}^\top \tag{A8}$$

$$\begin{aligned}\sum_{j\in C}(\kappa_v(y_j^* - \mathrm{avg}((y_k^*)_{k\in C}))(y_j - \mathrm{avg}((y_k)_{k\in C}))^\top + \kappa_M Z_j^* Z_j^\top) \\ = \bar{U}\overline{S}\overline{V}^\top\end{aligned} \tag{A9}$$

where $\overline{S} = \mathrm{diag}(\overline{\sigma}_1, \ldots, \overline{\sigma}_d)$. From Equations (27) and (A9),

$$\begin{aligned}\bar{U}\overline{S}\overline{V}^\top &= \sum_{j\in C}(\kappa_M R^* R_j^*(RR_j)^\top \\ &\quad + \kappa_v(R^* x_j^* - \mathrm{avg}((R^* x_k^*)_{k\in C}))(Rx_j - \mathrm{avg}((Rx_k)_{k\in C}))^\top) \\ &= \sum_{j\in C} R^*(\kappa_v(x_j^* - \mathrm{avg}((x_k^*)_{k\in C}))(x_j - \mathrm{avg}((x_k)_{k\in C}))^\top \\ &\quad + \kappa_M R_j^* R_j^\top\} R^\top \\ &= R^*\hat{U}\hat{S}\hat{V}^\top R^\top = (R^*\hat{U})\hat{S}(R\hat{V})^\top\end{aligned} \tag{A10}$$

is derived, which leads to $\overline{S} = \hat{S}$, $\overline{V} = R\hat{V}$, and $\hat{U} = R^*\bar{U}$. Then, from Equations (27) and (A8),

$$\begin{aligned}\overline{R}_C &= (R\hat{V})\mathrm{diag}(1, \ldots, 1, \det((R\hat{V})(R^*\hat{U})^\top))(R^*\hat{U})^\top \\ &= R\hat{R}_C(R^*)^\top\end{aligned} \tag{A11}$$

is derived. From Equations (29) and (A11), we obtain

$$\begin{aligned}\frac{\partial\hat{v}_C}{\partial R_i}((R(R_j, x_j + \tau), R^*(R_j^*, x_j^* + \tau^*))_{j\in C}) \\ = \kappa_M((RR_i) - \overline{R}_C(R^* R_i^*)) \\ = \kappa_M R(R_i - \hat{R}_C R_i^*) \\ = R\frac{\partial v}{\partial R_i}((R_j, x_j, R_j^*, x_j^*)_{j\in C})\end{aligned}$$

which leads to (31). (32) can be derived in the same way.

Proof of Lemma 7

From Equations (25) and (30),

$$\begin{aligned}\sum_{i\in\mathcal{V}}\frac{\partial v_C}{\partial x_i} &= \kappa_v\sum_{i\in\mathcal{V}}\sum_{k\in\mathrm{clq}_i(G)}(x_i - \mathrm{avg}((x_j)_{j\in C_k}) \\ &\quad - \hat{R}_C(x_i^* - \mathrm{avg}((x_j^*)_{j\in C_k}))) \\ &= \kappa_v\sum_{k\in\mathrm{clq}(G)}\sum_{i\in C_k}(x_i - \mathrm{avg}((x_j)_{j\in C_k}) \\ &\quad - \hat{R}_C(x_i^* - \mathrm{avg}((x_j^*)_{j\in C_k}))) = 0\end{aligned}$$

is obtained. From this, (9), (16), and (22),

$$\frac{d(\sum_{i\in\mathcal{V}} x_i(t))}{dt} = \sum_{i\in\mathcal{V}}\dot{x}_i(t) = \sum_{i\in\mathcal{V}}\frac{\partial v_C}{\partial x_i} = 0$$

is obtained. Hence, (14) holds.

Proof of Lemma 8

Consider $(\tilde{R}_i, \tilde{x}_i)_{i\in\mathcal{V}} \in \upsilon^{-1}(0)$. Then, from Equations (22), (23), and (24), the following holds for any $C \in \mathrm{clq}(G)$:

$$\exists(\hat{R}_C, \hat{\tau}_C) \in \mathrm{SE}(d) \text{ s.t. } (\tilde{R}_j, \tilde{x}_j) = (\hat{R}_C R_j^*, \hat{R}_C x_j^* + \hat{\tau}_C)\ \forall j \in C \quad \text{(A12)}$$

Assume that G is connected. From Lemma 3, $\upsilon^{-1}(0) \supset \mathcal{T}((R_i^*, x_i^*)_{i\in\mathcal{V}})$ is obtained. We show the converse inclusion to prove (18). Because G is connected, there is a sequence of cliques $(C_1, C_2, \ldots, C_q)$ for a positive integer $q \geq |\mathrm{clq}(G)|$ such that $C_k \cap C_{k+1}$ is non-empty for $k = 1, 2, \ldots, q-1$ and $\bigcup_{k=1}^{q} C_k = \mathcal{V}$. Let $j_k \in C_k \cap C_{k+1}$, and from Equation (A12), $\hat{R}_{j_k}(R_{j_k}^*)^\top = \hat{R}_{C_k} = \hat{R}_{C_{k+1}}$ holds. Then, from Equation (A12), $\tilde{x}_{j_k} - \hat{R}_{C_k} x_{j_k}^* = \hat{\tau}_{C_k} = \hat{\tau}_{C_{k+1}}$ holds. Hence, all $(\hat{R}_{C_k}, \hat{\tau}_{C_k})$ are equal to some $(\hat{R}, \hat{\tau}) \in \mathrm{SE}(d)$. Then, from Equation (A12), $(\tilde{R}_j, \tilde{x}_j) = (\hat{R}R_j^*, \hat{R}x_j^* + \hat{\tau})$ holds for any $j \in \mathcal{V}$, which indicates $(\tilde{R}_j, \tilde{x}_j)_{j\in\mathcal{V}} \in \mathcal{T}((R_i^*, x_i^*)_{i\in\mathcal{V}})$ from Equation (12). Hence, $\upsilon^{-1}(0) \subset \mathcal{T}((R_i^*, x_i^*)_{i\in\mathcal{V}})$ holds, and (18) is achieved.

If G is not connected, there is no such sequence of cliques $(C_1, C_2, \ldots, C_q)$. Then, not all $(\hat{R}_{C_k}, \hat{\tau}_{C_k})$ are equal, and from Equation (A12), $(\tilde{R}_j, \tilde{x}_j)_{j\in\mathcal{V}} \notin \mathcal{T}((R_i^*, x_i^*)_{i\in\mathcal{V}})$ holds, which indicates that (18) does not hold.

Proof of Lemma 9

We just have to show the boundedness of $x_i(t)$ for every $i \in \mathcal{V}$. Consider a connected graph G without loss of generality. Otherwise, we just have to consider each connected component of G. From Lemma 7, $\|\sum_{i\in\mathcal{V}} x_i(t)\|$ is bounded. From Equation (A1), the following holds:

$$\upsilon_\star((R_i(t), x_i(t))_{i\in\mathcal{V}}) \leq \upsilon_\star((R_i(0), x_i(0))_{i\in\mathcal{V}}) \quad \text{(A13)}$$

Without loss of generality, assume that agents $1, 2 \in C$ for a maximal clique C. From Equations (22), (25), and (26),

$$\begin{aligned}
&\frac{2}{\kappa_\upsilon}\upsilon_\star((R_i, x_i)_{i\in\mathcal{V}}) \geq \frac{2}{\kappa_\upsilon}\upsilon_C((R_i, x_i)_{i\in C}) \\
&= \sum_{j\in C}\left(\frac{\kappa_M}{\kappa_\upsilon}\|R_j - \hat{R}_C R_j^*\|^2 + \|x_i\right. \\
&\quad \left. -\mathrm{avg}((x_k)_{k\in C}) - \hat{R}_C(x_i^* - \mathrm{avg}((x_k^*)_{k\in C}))\|^2\right) \\
&\geq \|x_1 - \mathrm{avg}((x_k)_{k\in C}) - \hat{R}_C(x_1^* - \mathrm{avg}((x_k^*)_{k\in C})\|^2 \\
&\quad + \|x_2 - \mathrm{avg}((x_k)_{k\in C}) - \hat{R}_C(x_2^* - \mathrm{avg}((x_k^*)_{k\in C})\|^2 \\
&\geq \frac{1}{2}\|x_1 - x_2 - \hat{R}_C(x_1^* - x_2^*)\|^2 \\
&\geq \frac{1}{2}(\|x_1 - x_2\| - \|x_1^* - x_2^*\|)^2
\end{aligned} \quad \text{(A14)}$$

is derived. From Equations (A13) and (A14),

$$\|x_1(t) - x_2(t)\| \leq 2\sqrt{\frac{\upsilon_\star((R_i(0), x_i(0))_{i\in\mathcal{V}})}{\kappa_\upsilon}} + \|x_1^* - x_2^*\| \quad \text{(A15)}$$

is obtained for $t \geq 0$. Equation (A15) implies that $\|x_1(t) - x_2(t)\|$ is bounded. The boundedness of $\|x_i(t) - x_j(t)\|$ for any $i, j \in \mathcal{N}$ is guaranteed because G is connected. With this fact, the following inequality shows the boundedness of $x_i(t)$:

$$\begin{aligned}
\|x_i(t)\| &\leq \left\|x_i(t) - \frac{1}{n}\sum_{j\in\mathcal{V}} x_j(t)\right\| + \left\|\frac{1}{n}\sum_{j\in\mathcal{V}} x_j(t)\right\| \\
&\leq \frac{1}{n}\sum_{j\in\mathcal{V}}\left\|x_i(t) - x_j(t)\right\| + \frac{1}{n}\left\|\sum_{j\in\mathcal{V}} x_j(t)\right\|
\end{aligned}$$

Proof of Lemma 10

As for (17), $((\mathcal{P}_{\mathrm{skew}}(R_i^\top(\partial\upsilon/\partial R_i)), (\partial\upsilon/\partial x_i))_{i\in\mathcal{V}})^{-1}(0) \supset \upsilon^{-1}(0)$ is obvious. We show the converse inclusion for $\upsilon = \upsilon_\star$ in Equation (22). Since $\mathrm{SE}(d)$ is an analytic manifold, $\mathcal{T}((R_j^*, x_j^*)_{j\in\mathcal{V}})$ is an analytic manifold from Equation (12), and so is $\mathcal{P}_C(\mathcal{T}((R_j^*, x_j^*)_{j\in\mathcal{V}}))$ from Equation (3). Hence, the distance function $\upsilon_C((R_j, x_j)_{j\in C})$ in Equation (23) is analytic on an open set around $\upsilon_C^{-1}(0)$ [38, 39]. Therefore, $\upsilon_\star$ in Equation (22) is analytic on an open set $\hat{\mathcal{O}} \subset (\mathrm{SE}(d))^n$ around $\bigcup_{C\in\mathrm{clq}(G)} \upsilon_C^{-1}(0) = \upsilon_\star^{-1}(0)$. Hence, Lojasiewicz's inequality [40, 41] (the Riemannian manifold version [42]) is available: For every $(\tilde{R}_j, \tilde{x}_j)_{j\in\mathcal{V}} \in \upsilon_\star^{-1}(0)$, there exist a bounded open set $\Omega = \Omega((\tilde{R}_j, \tilde{x}_j)_{j\in\mathcal{V}}) \subset \hat{\mathcal{O}}$ containing $(\tilde{R}_j, \tilde{x}_j)_{j\in\mathcal{V}}$, $\beta = \beta((\tilde{R}_j, \tilde{x}_j)_{j\in\mathcal{V}}) > 0$, and $\theta = \theta((\tilde{R}_j, \tilde{x}_j)_{j\in\mathcal{V}}) > 0$ such that

$$\begin{aligned}
\upsilon_\star((R_j, x_j)_{j\in\mathcal{V}}) \leq \beta\Bigg(\sum_{i\in\mathcal{V}}\Bigg(&\left\|\left(\mathcal{P}_{\mathrm{skew}}\left(R_i^\top\frac{\partial\upsilon_\star}{\partial R_i}((R_j, x_j)_{j\in\mathcal{V}})\right)\right)\right\|^2 \\
&+\left\|\frac{\partial\upsilon_\star}{\partial x_i}((R_j, x_j)_{j\in\mathcal{V}})\right\|^2\Bigg)\Bigg)^\theta \quad \forall (R_j, x_j)_{j\in\mathcal{V}} \in \Omega
\end{aligned} \quad \text{(A16)}$$

Let $\mathcal{O} = \bigcup_{(\tilde{R}_j, \tilde{x}_j)_{j\in\mathcal{V}} \in \upsilon_\star^{-1}(0)} \Omega((\tilde{R}_j, \tilde{x}_j)_{j\in\mathcal{V}})$, and $\mathcal{O}$ is an open set satisfying $\mathcal{O} \supset \upsilon_\star^{-1}(0)$. Then, (A16) indicates that $((\mathcal{P}_{\mathrm{skew}}(R_i^\top(\partial\upsilon_\star/\partial R_i)), (\partial\upsilon_\star/\partial x_i))_{i\in\mathcal{V}})^{-1}(0) \cap \mathcal{O} \subset \upsilon_\star^{-1}(0)$, and (17) is achieved for $\upsilon = \upsilon_\star$.